

# Past and future climate change effects on thermal regime and oxygen solubility of four peri-alpine lakes

Authors: Olivia Desgué-Itier<sup>1,4</sup>, Laura Melo Vieira Soares<sup>1</sup>, Orlane Anneville<sup>1</sup>, Damien Bouffard<sup>2</sup>, Vincent Chanudet<sup>3</sup>, Pierre Alain Danis<sup>4,5</sup>, Isabelle Domaizon<sup>1</sup>, Jean Guillard<sup>1</sup>, Théo Mazure<sup>1</sup>, Najwa Sharaf<sup>4,5</sup>, Frédéric Soullignac<sup>6</sup>, Viet Tran-Khac<sup>1</sup>, Brigitte Vinçon Leite<sup>7</sup>, Jean-Philippe Jenny<sup>1</sup>

<sup>1</sup>Université Savoie Mont Blanc, INRAE, CARRTEL, 74200 Thonon-les-Bains, France

<sup>2</sup>Eawag, Swiss Federal Institute of Aquatic Science and Technology, Surface Waters – Research and Management, 6047 Kastanienbaum, Switzerland

<sup>3</sup>EDF, Hydro Engineering Centre, Environment and Social Department, 73290 La Motte Servolex, France

<sup>4</sup>Pôle R&D « Ecla », INRAE, 3275 Route Cézanne, 13182 Aix-en-Provence, France<sup>5</sup>Office Français de la Biodiversité, Unité « Ecla », INRAE, Aix-en-Provence, France

<sup>5</sup>INRAE, Aix Marseille Univ, RECOVER, Team FRESHCO, 3275 Route Cézanne, 13182 Aix-en-Provence, France

<sup>6</sup>CIPEL, International Commission for the protection of the waters of Lake Geneva, 1260 Nyon, Switzerland

<sup>7</sup>Laboratoire Eau, Environnement, Systèmes Urbains (LEESU), École Nationale des Ponts et Chaussées, Marne-la-Vallée, France

*Correspondence to:* Olivia Desgué-Itier (olivia.desgue@inrae.fr); Jean-Philippe Jenny (Jean-Philippe.Jenny@inrae.fr)

**Abstract.** Climate change modifies the thermal regime and the oxygen solubility of lakes globally, resulting in the alteration of ecosystem processes, lake habitats and concentrations of key substances. The use of one-dimensional (1D) lake model for global scale studies has become the standard in lake research to evaluate the effects of climate change. However, such approach requires global scale forcing variables which have several limitations that are barely discussed, such as the need of serious downscaling. Furthermore, projections of lakes' thermal regime are hardly ever confronted with long-term observations that extent for more than a few decades. These shortfalls limit the robustness of hindcast/ forecast simulations on decadal to centennial timescales. In this study, several 1D lake models' robustness was tested for long-term variations based on 63 years of limnological data collected by the French Observatory of LAkes (OLA). Here we evaluate the possibility to force mechanistic models by following the long-term evolution of shortwave radiation and air temperature while providing realistic seasonal trend for the other variables for which local scale downscaling often lacks accuracy. Then, the effects of climate change on the thermal regime and oxygen solubility were analyzed in the four-largest French peri-Alpine lakes. Our results show that Mylake, the best performing of the five 1D tested models for the four study sites, forced by air temperatures and short-wave radiations accurately predict variations in lake thermal regime over the last four to six decades, with RMSE < 1.95 °C. During the last three decades, water temperatures have increased by 0.46 °C decade<sup>-1</sup> (±0.02 °C) in the epilimnion and 0.33 °C decade<sup>-1</sup> (±0.06 °C) in the hypolimnion. Concomitantly and due to thermal change, O<sub>2</sub> solubility has decreased by -0.104 mg L<sup>-1</sup> decade<sup>-1</sup> (±0.005 mg L<sup>-1</sup>) and -0.096 mg L<sup>-1</sup> decade<sup>-1</sup> (±0.011 mg L<sup>-1</sup>) in the epilimnion and hypolimnion, respectively. Based on the ssp370 socio-economic pathway of the IPCC, perialpine lakes could face an increase of 3.80 °C (±0.20 °C) in the next 70 years, accompanied by a decline of 1.0 mg L<sup>-1</sup> (±0.1 mg L<sup>-1</sup>) of O<sub>2</sub> solubility. These results suggest important degradation in lake thermal and oxygen conditions and a loss of habitats for endemic species.

## 1 Introduction

Lakes are critical resources providing humanity with many ecosystem services such as hydropower and drinking water production (Jenny et al., 2020) and are considered sentinels of climate change (Williamson et al., 2009). Nevertheless, the alteration of these ecosystems under anthropogenic pressures and ongoing global warming requires continuous water quality monitoring. Lake water temperature is a critical indicator for long-term monitoring of lake ecosystems and for adapting better management practices for preservation (Daufresne et al., 2009). It is an important parameter impacting the metabolism, composition, and functioning of lake ecosystems as well as reflecting their response to climate change. Water temperature has

45 a direct effect on the speed of development, growth rate and reproduction rate of aquatic organisms (Angellita et al., 2003 ;  
Mari et al., 2016a) and on phenology (Parmesan, 2006 ; Walter et al., 2002). Furthermore, water temperature can also indirectly  
affect organisms, by altering the mixing regime of lakes and governing gas solubility with potential impacts on oxygenation  
conditions, one of the most fundamental parameters of life in lakes (Roberts et al., 2009a; Wetzel, 2001a).

Recent global studies from lakes around the world have already shown that increasing air temperature has a significant  
50 effect on the intensification and the duration of stratification (Woolway and Merchant, 2019; Piccioni et al., 2021; Woolway  
et al., 2021). In deep temperate lakes, vertical mixing of the water column has experienced a decrease in intensity, frequency,  
and duration (Råman Vinnå et al., 2021; Danis et al., 2004), thereby increasing the vertical temperature gradient between the  
surface and deep layers (Livingstone, 2003). However, the study of lakes' thermal regime over decadal to centennial timescales  
is still limited, hence precluding our understanding of the evolution of lake physicochemical conditions and habitats as well as  
55 the response mechanisms to the forcings involved over such timescales.

Mechanistic lake models have been widely implemented over the last years (Bruce et al., 2018a; Shatwell et al., 2019;  
Snortheim et al., 2017) and are considered as an essential tool for understanding, analyzing, testing different scenarios, and  
predicting the state of an ecosystem under external constraints over different timescales (Trolle et al., 2012). More specifically,  
the use of one-dimensional (1D) model for global scale studies has become the standard in lake research. These models are  
60 suitable to simulate complex ecosystems as they require minimum configuration parameters (Hamilton and Schladow, 1997;  
Vinçon-Leite et al., 2014), and to perform reliable predictions to study lakes responses to global warming (Balsamo et al.,  
2012). However, such approach requires global scale forcing parameters which has several limitations that are barely  
discussed. Among these limitations, the influence of the rivers and watersheds is not systematically assessed whereas it can  
have a strong effect on the change in the thermal structure of lakes with a short residence time (e.g <1-3 year) (Råman Vinnå  
65 et al., 2017, 2018; Perga et al., 2018). Another limitation relies on the quality of the forcing. Lakes are often smaller than the  
meteorological grid size used in studies. Some parameters such as wind can strongly vary at local scales especially in alpine  
regions. This issue is attimes tackled by using meteorological forcing downscaled to local weather stations (e.g. Råman Vinnå  
et al., 2021), or by trying to simplify the heat budget (e.g. Piccolroaz et al., 2013). The quality of the input data is also limiting  
the possibility to estimate changes in the thermal structure over very long trends (> 100 years). Models are in large extent  
70 calibrated against very few years of limnological records so far (Soares and Calijuri, 2021), potentially limiting the robustness  
of hindcast/ forecast exercises on long-term timescales such as pluri-decadal or pluri-centennial.

To address this limitation, the first aim of our study is to adapt an existing modeling approach for long-term studies,  
constrained by climate scenarios of the IPCC, and to calibrate and validate the model against up to 63 years of limnological  
records from four perialpine lakes monitored by the Observatory of LAKes (OLA) (Rimet et al., 2020): Geneva, Annecy,  
75 Bourget, and Aiguebelette. Here we evaluate the possibility to force mechanistic models by following the long-term evolution  
of **only** shortwave radiation ( $W.m^{-2}$ ) and air temperature ( $^{\circ}C$ ) while providing realistic seasonal trends for the other variables,  
such as wind speed, for which local scale downscaling often lacks accuracy **and present more uncertainties on the long-term.**  
**Moreover, this is supported by a previous study that showed that ~60 % of the observed warming of spring and summer lake**  
**surface temperatures were caused by increased air temperature and ~40 % by increased solar radiation (Schmid and Köster,**  
80 **2016).** We use unique long observation datasets to insure the robustness of our findings.

The second objective of this study is to investigate the evolution of the thermal regime and the solubility of oxygen,  
**as proxys for the species' habitats and their capacity to cope with temperature change (Kraemer et al., 2021),** in the lakes over  
1850-2100 to assess their different responses and sensitivity to global warming.

We begin 1) by describing our approach for long-term forecast/ hindcast based on a reduced number of meteorological  
85 forcing variables, then 2) by presenting the **MyLake** model calibration and validation over a relatively short period of 10 years,  
using both complete and reduced meteorological inputs, then 3) we test the method over longer timescales, i.e., against 37 to  
63 years of monitoring data, and finally 4) we explore trends in lake thermal regime through 15 physical indices, and we

estimate effects of climate change on the dissolved oxygen [solubility](#) in the four lakes over the 1850-2100 period using an ensemble of climate projections based on the Shared Socioeconomic Pathways (ssp126, ssp370, and ssp585) (Riahi et al., 2017a).

**Table 1.** Characteristics of the four study sites

	Geneva	Annecy	Bourget	Aiguebelette
Location	46°27'; 6°32'	45°86'; 6°17'	45°43'; 5°52'	45°33'; 5°48'
Mean/Max depth (m)	154/309	41/65	85/145	31/70
Area (km <sup>2</sup> )	581.3	27.59	44.5	5.45
Mean elevation (m.a.s.l.)	372	447	232	390
Residence time of water (yrs)	11.3	3.8	9	3.1
Mixing regime	mono-mero-mictic	monomictic	monomictic	monomictic
Trophic state	Mesotrophic	Oligotrophic	Oligo-mesotrophic	Oligo-mesotrophic

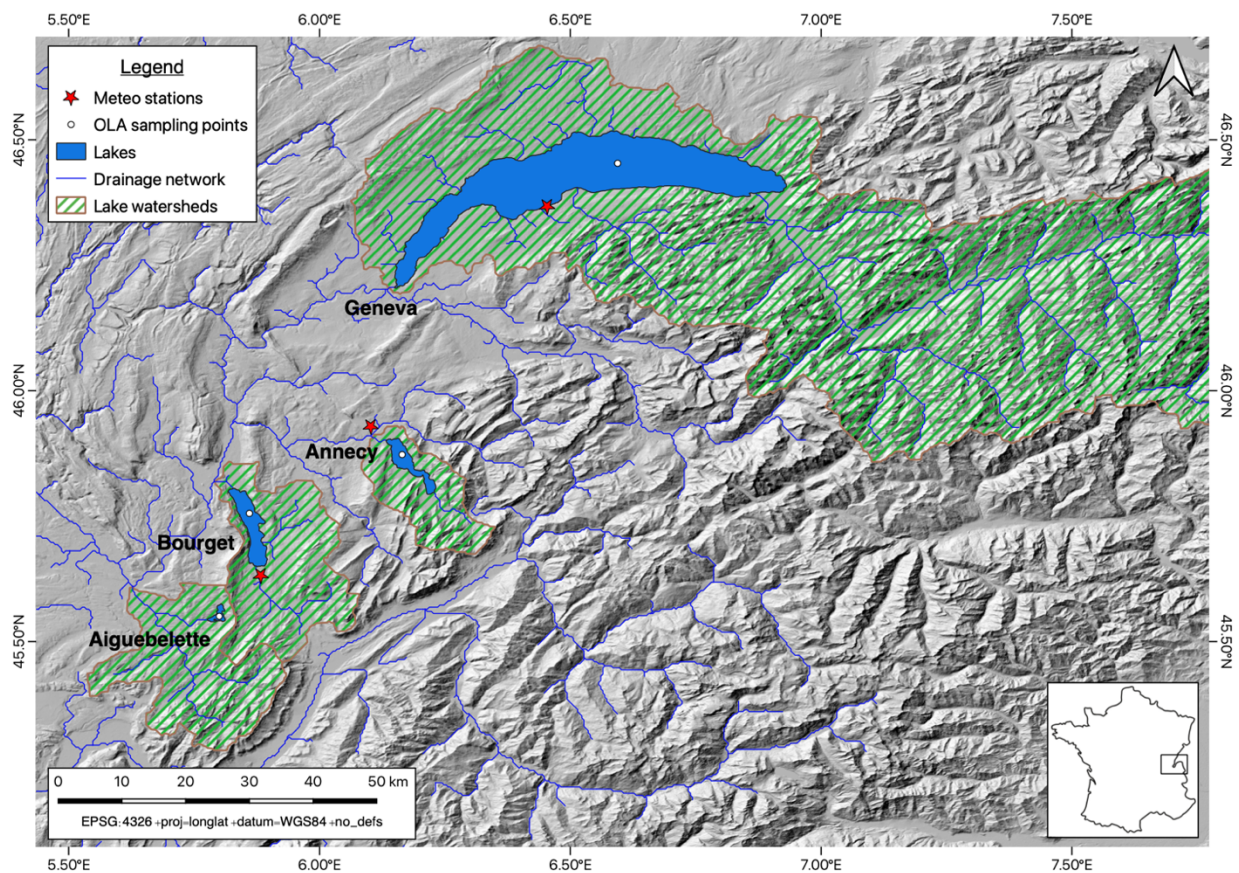


**Figure 1.** Location of the study sites in peri-alpine region. OLA sampling sites (Rimet et al., 2020), locations of meteorological stations, drainage watersheds, and networks are represented.

## 2 Methods

### 2.1 Study sites

We consider four lakes located in the peri-alpine region in France: Lake Geneva, Lake Annecy, Lake Bourget, and Lake Aiguebelette (Figure 1). They are situated in a continental mountain climate, and less than 150 km separate the four lakes from each other. The four lakes are mono [or meromictic](#) – they mix only once per year –, deep and of glacial origin. Lake



Geneva and Lake Aiguebelette are mesotrophic lakes, whereas Lake Annecy and Lake Bourget are oligotrophic and oligo-mesotrophic, respectively (Table 1).

## 105 2.2 Lake data

The Observatory of LAkes (OLA) managed by the CARRTEL ([https://si-ola.inra.fr/si\\_lacs/login.jsf](https://si-ola.inra.fr/si_lacs/login.jsf)) has regularly monitored the physical and chemical conditions of peri-alpine lakes. Limnological data derived from the OLA observatory databases provides several decades (from 37 to 63 years) (Table 5) of monitoring on lake thermal conditions, i.e., water temperatures along the water column in the pelagic zone. The study sites were monitored for up to six decades by CARRTEL. Measurements were recorded at the deepest point of each lake, generally twice a month from March to November and once a month during the rest of the year, except for Lake Aiguebelette which is monitored 6 times a year.

## 2.3 Hydrodynamic modelling

A modeling approach was performed to run five one-dimensional hydrodynamic lake models simultaneously (FLake, GLM, GOTM, Simstrat and MyLake) to simulate the vertical water temperature profile in the four perialpine lakes. The same configuration and driver data were used for each lake to account for different sources of uncertainties in the model predictions. We used the R package LakeEnsemblR version 1.0.0. (Moore et al., 2021). The models were calibrated and validated against OLA limnological data, and further used to assess long-term trends in the thermal regime of each lake. The MyLake model, identified as the most performant for the four peri-alpine lakes based on five performance metrics calculated, was selected to develop and test our approach for long-term reconstruction that extends the simulation period beyond the instrumental one, as this model is well adapted to Northern and alpine regions (Couture et al., 2018; Kobler and Schmid, 2019; Saloranta, 2006). MyLake was developed by the Norwegian Institute for Water Research (NIVA), the University of Helsinki (Finland) and Université Laval (Canada). It simulates daily vertical water temperature profiles, density stratification, seasonal ice and snow cover, sediment-water dynamics, and phosphorus-phytoplankton interactions (Saloranta and Andersen, 2007a).

## 2.4 Climate warming scenarios

The model was forced with statistically bias-adjusted (Lange, 2019a) and downscaled climate projections (Cucchi et al. 2020; Lange 2019b) (ISIMIP3BASD method) from phase 3b of the Inter-Sectoral Impact Model Intercomparison Project (ISIMIP3b). This was based on the output of phase 6 of the Coupled Model Intercomparison Project (CMIP6 (Eyring et al., 2016)). The better-performing models, providing daily data for all variables during the period of interest (1850-2100) were selected (Lange, 2019a) (GFDL-ESM4, IPSL-CM6-LR, UKESM1-0-LL, MPI-ESM1-2-HR and MRI-ESM2-0 (Table S2)) and compared to meteorological station data.

All five climate models were downscaled at 0.5° (55km) resolution. These models are good representatives of the entire CMIP6 ensemble as they are characterized with low (GFDL-ESM4, MPI-ESM1-2-HR, MRI-ESM2-0) and high climate sensitivity (IPSL-CM6A-LR, UKESM1-0-LL). The aim of the study being the reducing of model input variables to only those with the highest level of confidence on the long-term, such as air temperature and downwelling shortwave radiation, these two variables from each model were compared to available observation data from a meteorological station located at Thonon-les-bains (1987-2019 and 1971-2019 for air temperature and shortwave radiation, respectively) (Monitoring data from the INRAE CLIMATIK platform (<https://agroclim.inrae.fr/climatik/>, in French) managed by the AgroClim laboratory of Avignon, France). The model data were collected from the historical (1850-2014) and the intermediate (ssp370: 2015-2100) scenarios, in order to cover the entire period with available observation data. Only years with more than 350 days of data available were considered. Annual means and daily means during the monitoring periods were calculated and compared between modelled



and observed data. Three error assessment metrics (root mean squared error – RMSE, normalized mean absolute error – NMAE and Pearson correlation coefficient –  $r$ ) were calculated to evaluate the performance of climatic models. The most performant of the 5 models (IPSL-CM6A-LR) was selected and used as input data for the study.

145 CMIP6 experiments used were historical climate from 1850 to 2014, and scenarios ssp126 (SSP1-RCP2.6 climate), ssp370 (SSP3-RCP7 climate), and ssp585 (SSP5-RCP8.5 climate) from 2015 to 2100. The SSPs consider how societal choices will affect greenhouse emissions, [SSP126](#) being the most sustainable scenario and [SSP585](#) the worst one (Riahi et al., 2017b). The Representative Concentration Pathways (RCPs) corresponds to the range of the year 2100's radiative forcings values, from 2.6 to 8.5  $W m^{-2}$  (van Vuuren et al., 2011).

## 150 2.5 Meteorological forcing data

The meteorological forcing variables required in the *LakeEnsemblR* package are air temperature ( $^{\circ}C$ ), downwelling shortwave radiation ( $W m^{-2}$ ), 10-m elevation wind speed ( $m s^{-1}$ ), cloud cover fraction, relative humidity (%), rain ( $mm.day^{-1}$ ), and surface-level barometric pressure (Pa), at a daily time step.

From the chosen climate model (IPSL-CM6-LR), all forcing variables were extracted for the grid cells containing the  
155 four lakes, Lakes Bourget and Aiguebelette being situated in the same grid. A sensitivity test was carried out on all seven climate variables to validate our hypothesis that forcing variables can be reduced into the hydrodynamic models to only air temperature and shortwave radiations to identify long-term trends accurately (Table S1). [Each climate forcing variables \(air temperature, downwelling shortwave radiation, wind speed, cloud cover, relative humidity, rain and surface pressure\)](#) was tested from MyLake water temperature simulations over a 10-year period, for the 4 perialpine lakes. A percentage of  $\pm 20\%$   
160 was added to each climate variable daily values and then the performance metrics (RMSE and  $R^2$ ) were calculated from model outputs and observation data. The difference between model performance with raw data and after applying the 20% coefficient to the input values was calculated. Variables with the greatest variation of its performance metrics were identified as variables with the most important effect on MyLake model performance.

Then, simulations with the MyLake model for the four lakes were computed with four different climatic  
165 configurations: (i) with only air temperature and shortwave radiation from ISIMIP3b while all other variables were extracted from meteorological observations from which daily means were calculated and replicated every year from 1850 to 2100; (ii) with all input meteorological forcing variables extracted from ISIMIP3b. The period of meteorological observations extends from 2000 to 2011 for Lake Geneva (MétéoSuisse Data Warehouse) and from 1959 to 2020 for the other lakes (Table 4) (SAFRAN climatic data are provided by Météo-France and were downloaded via the SICLIMA platform developed by  
170 AgroClim-INRAE). Decoupling meteorological parameters is a strong assumption, which is addressed in the discussion section. The cloud cover was available only for Lake Geneva, and values were adopted as the same for the other lakes. Surface pressure was considered constant in this study. [Configurations \(iii\) and \(iv\)](#) are based on configurations (i) and (ii) respectively, with a correction factor for both air temperature and shortwave radiation (Table 2). These two variables were compared to available data from the closest meteorological stations (from INRAE and Meteo France networks – CLIMATIK and SAFRAN  
175 database), encompassing 32 to 61 years of meteorological time series data (Fig. 1) (Table 3). Correction factors were calculated from the difference between raw climatic model data and observed data from local stations, at the daily resolution, to fit better to meteorological data and correct the altitude bias (Fig. S2; Fig. S3). Further, daily corrected meteorological data were used between 1850 and 2100.

180 **Table 2. Meteorological forcing configuration and performance metrics** for MyLake (ISIMIP) calculated between daily simulations and observations. Outputs comparison between 4 configurations: (i) [only air temperature \( \$T^{\circ}C\$ \) and shortwave radiation \(Sw\) extracted from ISIMIP3B without a correction factor](#) and others from meteorological observations (ii) all

ISIMIP3b forcing data with no correction factor, (iii) only air T°C and Sw extracted from ISIMIP3B with a correction factor, (iv) all ISIMIP3b forcing data with a correction factor applied to air T°C and Sw, over a ten-year period.

Configuration	Inputs variables	Lake	RMSE (°C)	Pearson_r	Bias	MAE	NSE
(i)	Air T°C and Sw No correction factor	Geneva	1.583	0.957	-1.02	1.557	0.842
		Annecy	2.686	0.933	-1.930	1.989	0.667
		Bourget	1.389	0.960	0.902	1.110	0.863
		Aiguebelette	2.290	<b>0.950</b>	1.825	2.012	0.764
(ii)	ALL forcing data No correction factor	Geneva	1.398	0.955	0.739	1.028	0.877
		Annecy	1.972	<b>0.945</b>	-0.882	<b>1.215</b>	0.821
		Bourget	2.233	0.948	1.887	2.015	0.646
		Aiguebelette	3.200	0.945	2.760	2.878	0.576
(iii)	Air T°C and Sw with correction factor	Geneva	<b>1.143</b>	<b>0.961</b>	<b>0.302</b>	<b>0.727</b>	<b>0.918</b>
		Annecy	1.951	0.938	-0.992	1.270	0.824
		Bourget	<b>1.022</b>	<b>0.963</b>	<b>-0.046</b>	<b>0.620</b>	<b>0.926</b>
		Aiguebelette	<b>1.587</b>	0.949	<b>0.305</b>	<b>1.138</b>	<b>0.896</b>
(iv)	ALL forcing data with correction factor	Geneva	2.144	0.949	1.551	1.619	0.710
		Annecy	<b>1.699</b>	0.942	<b>0.331</b>	1.277	<b>0.867</b>
		Bourget	1.532	0.958	1.055	1.300	0.834
		Aiguebelette	2.050	<b>0.948</b>	1.296	1.655	0.827

185

**Table 3.** Meteorological data sources used to calculate the correction factors applied to Air temperature (T°C) and Shortwave radiations, for the 4 study sites.

	Lake Geneva	Lake Annecy	Lake Bourget	Lake Aiguebelette
Data base	CLIMATIK - INRAE	CLIMATIK – Meteo France	SAFRAN	SAFRAN
Station	Thonon-les-Bains	Meythet	Voglans	Voglans
Period	Air T°C : 1987-2019	Air T°C : 1993-2019	Air T°C : 1959-2020	Air T°C : 1959-2020
	Shortwave : 1971-2019	Shortwave : 2010-2017	Shortwave : 1959-2020	Shortwave : 1959-2020

190

Daily meteorological data from the SAFRAN analysis system were extracted from SICLIMA data base (Pagé, 2008), collected by Meteo France since January 1<sup>st</sup> of 1959. Data have been re-calculated from daily local observations at smaller grid cells (8km x 8km) by Meteo France.

**Table 4.** Meteorological data sources used for the meteorological patterns calculated from daily means of Cloud cover (Cl), Relative humidity (Rh), Wind speed (Ws) and Rain (R) variables, for the 4 study sites.

	Lake Geneva	Lake Annecy	Lake Bourget	Lake Aiguebelette
Data base	MétéoSuisse	SAFRAN (Rh,Ws,R) MétéoSuisse (Cl)	SAFRAN (Rh,Ws,R) MétéoSuisse (Cl)	SAFRAN (Rh,Ws,R) MétéoSuisse (Cl)
Station	Nyon/Changins	Meythet Nyon/Changins	Voglans Nyon/Changins	Voglans Nyon/Changins
Period	2000-2011	1959-2020 (Rh,Ws,R)	1959-2020 (Rh,Ws,R)	1959-2020 (Rh,Ws,R)
		2000-2011 (Cl)	2000-2011 (Cl)	2000-2011 (Cl)

## 2.6 Model set-up, calibration, and validation

195

MyLake was run through the package *LakeEnsemblR package*. The model was calibrated considering the most sensitive parameters identified in previous studies (Saloranta, 2006): scaling factors for wind speed and shortwave radiation and physical C\_shelter parameter. The Latin Hypercube Calibration (LHC) method was used for calibration. The LHC method uses upper and lower bounds for all parameters considered, and then samples evenly within the parameter space given by these

bounds. Then MyLake was run and evaluated for 100 parameters sets. The performance of the model was assessed through  
200 six statistical metrics: RMSE, Nash-Sutcliffe efficiency (NSE), r, bias, MAE and NMAE.

The optimal values of model parameters were determined based on the performance metrics. First, calibration and  
validation were performed over a period of 10 years, depending on the density of observation data for each lake. This period  
corresponds to the temporal scale generally covered by modeling studies performed between 2015 to 2020 (Soares and Calijuri,  
2021) (Table 5). Further, the robustness of the model to perform long-term simulations was assessed by computing the  
205 performance metrics over the complete period with field data availability, covering 63, 54, 37, and 46 years for Lakes Geneva,  
Annecy, Bourget, Aiguebelette, respectively (Table 5).

For the long-term simulations according to the three scenarios (from 1850 to 2100), initial water temperature remained  
unknown. To address this limitation, a method was developed to identify the year with available observation data, the closest  
from climatic conditions estimated in January 31<sup>st</sup> 1850. Air temperature from 1<sup>st</sup> to 31<sup>st</sup> January 1850 was compared to air  
210 temperature of the instrumental period (from OLA database) to identify years with similar climate conditions. The water  
temperature profile of the year with the lowest RMSE between winter air temperatures (1992 for Lakes Bourget and Geneva -  
2000 for Lakes Annecy and Aiguebelette) was used as the initial profile, 31<sup>st</sup> of January 1850.

215 **Table 5.** Monitoring, calibration and validation periods for the four peri-alpine lakes

	Geneva	Annecy	Bourget	Aiguebelette
Monitoring	1957-2020	1966-2020	1984-2021	1974-2020
Calibration	1980-1990	1970-1980	1998-2008	1995-2005
Validation	1990-2000	2000-2010	2008-2018	2005-2015
Long-term validation	1957-2018	1966-2020	1984-2018	1974-2020

## 2.7 Assessment of lakes response to warming

Model fit was assessed for 15 thermal indices: lake temperature (full profile), surface temperature (**Ts at 5m**), bottom  
temperature (**Tb at 60 m, 60 m, 299 m and 140 m** for Lakes Annecy, Aiguebelette, Geneva, and Bourget, respectively), mean  
220 temperature along the water column (**Tm**), metalimnion depth (top and bottom) defined as the water stratum with the steepest  
thermal gradient, demarcated by the bottom of the epilimnion and top of the hypolimnion (Wetzel, 2001b), epilimnion  
temperature, hypolimnion temperature, Schmidt stability (Idso, 1973), buoyancy frequency (Brunt-Vaisala frequency),  
thermocline depth and stratification characteristics (start, end, duration, maximum intensity and day of the year) (See  
supplementary). The R package rLakeAnalyzer (Winslow et al., 2019) was used to calculate epilimnion **extent and**  
225 **temperature, hypolimnion extent and temperature, metalimnion upper and lower depths**, Schmidt stability, buoyancy frequency  
and thermocline depth. The dates of stratification onsets/break-ups were defined as the day when the surface-to-bottom  
temperature differences were greater or less than 2 °C (Robertson and Ragotzkie, 1990) for at least 5 consecutive days. **The**  
**stratification duration was calculated as the period between the day of onset and break-up, as defined above.** The maximum  
stratification intensity was defined as the greatest difference between Ts and Tb. Water volumes above certain thresholds of  
230 ecological interest (7 °C, 9 °C and 12 °C) (Wolfe, 1996) above which the reproduction, growth, and survival of certain fish  
species may be affected (Mari et al., 2016b; Réalis-Doyelle, 2016) were calculated from bathymetry files. Finally, potential  
oxygen solubility was calculated as a function of water temperature following Winkler Table.

## 2.8 Statistical analysis

The slope of the significant trends was evaluated by least-squares linear regression and t-tests when followed a normal  
235 distribution. Otherwise, the non-parametric Mann-Kendall test and the Theil-Sen method were used to estimate if the slope



was significant and provide the slope's value. The Shapiro-Wilk test and Fisher's F test evaluated the distribution normality and variance homoscedasticity, respectively. Average values of each thermal metric in present (1990-2020) and future (2070-2100) were compared with either the Student t mean difference test in case of residuals normal distribution and homoscedasticity or the Welsh t mean difference test when variances were different. When normal [distribution of residuals](#) was not followed, the Mann-Whitney U test (equal variances) or the Kolmogorov-Smirnov test (different variances) were used instead. A p-value of 0.05 was used to represent the significance of the statistical tests. Kernel densities were calculated to compare averaged daily data distribution over 2000-2010 and 2090-2100. The coefficient of overlap of the two distributions was calculated (Ridout and Linkie, 2009). The analyses were carried out with the R software (version 4.1.2, R Core Team, 2021).

## 245 **3 Results**

### **3.1 Model performance**

The MyLake model, forced by air temperature and shortwave radiation, reproduced well the observed temperature along the water column in the four deep alpine lakes (Fig. 2). Model performances were compared across a 10-year validation and more extended periods (Table 6), depending on the availability of observations for each lake. During both validation periods (i.e., 10 years and the 37-63 years period), the model predicted water temperature with good precision, as RMSE values are generally less than 2 °C and 1.22 °C for the two deepest lakes (Geneva and Bourget). The model reproduced well the inter-annual temperature variability of the four lakes (Fig. 3) with Pearson correlation coefficient values ( $r$ ) >0.9 over the 10-year calibration and validation periods. The model robustness has been maintained over the long term as  $r$  values remained >0.9. Depending on the lake considered, the model either slightly underestimated the water temperature (bias = -0.03-0.05 °C and -0.91-0.99 °C for Lake Bourget and Annecy, respectively) or overestimated it (+0.31-+0.69 °C and +0.3 °C for Lakes Aiguebelette and Geneva respectively). These results showed that this is not a systematic tendency to over or underestimate the water temperature however depends on the lake characteristics.

The ability of the model to predict the evolution of specific thermal indices has been assessed (Table 7). The model performance in predicting epilimnion temperatures was the best for the two deepest lakes (Geneva and Bourget), with RMSEs ranging between 1.92 and 2.08 °C. For Lake Annecy, the discrepancies obtained for the epilimnion simulations were similar to those of the simulated temperature profiles over the 10-year validation period (RMSE=2.02 and 1.56 °C, respectively). Still, it was less effective over the long-term validation (RMSE=3.69 °C). Similarly, the model was more performant in predicting the epilimnion temperature of Lake Aiguebelette during the 10-year validation period (RMSE=2.61 °C) compared to the long-term validation (RMSE=4.6 °C). The epilimnion inter-annual variability of the four lakes was well reproduced, with  $R^2$ >0.89 and  $R^2$ >0.65 for the 10-year and long-term validations respectively.

A clear difference in amplitude has been identified between Schmidt stability calculated from simulations and observed water temperature profiles (mean RMSE = 3270.7, 4092.6, 3391.9, 1967.1 for Geneva, Bourget, Annecy, and Aiguebelette, respectively) however general seasonal patterns across the four lakes were well simulated by the model ( $R^2$ >0.86 for the 10-year and  $R^2$ >0.66 for the long-term validation periods). The average model performance between the two validation periods after comparing calculations of observed and simulated thermocline depth is found to be better for [Lakes Bourget and Aiguebelette](#) (with RMSE = 9.7, 9.1, 11.7 and 24.6 m for lakes Bourget, Aiguebelette, Annecy and Geneva, respectively). [When considering only the stratified summer period, from June to September, the MyLake model was more performant to predict the thermocline depth, especially in Lake Geneva and Aiguebelette](#) (with average RMSE = 6.4, 3.9, 7 and 8.4 m for [Lakes Geneva, Aiguebelette, Bourget and Annecy, respectively](#)). The RMSE associated with the prediction of the onset stratification was lower for Lake Bourget and Aiguebelette over the long-term validation period (RMSE=12.9 and 15.8 days, respectively) and less accurate for Lake Annecy and Geneva (RMSE=28.0 and 20.9 days, respectively). The estimation of the end-of-stratification date was reasonably close for Lake Bourget and Annecy (10.7<RMSE<13.4 days and 15.2<RMSE<18.9

280 days for 10-year and long-term validation periods respectively). The model predicted better the end-of-stratification for Lake Aiguebelette (RMSE=5.5/13.2 days) compared to Lake Geneva (RMSE=17.0/23.7 days). Moreover, the stratification duration was represented more accurately for Lake Bourget (RMSE=13.09 and 17.7 days for the 10-year and long-term validation periods, respectively) and ranges between one month and one month and a half for the other lakes ( $25.9 < \text{RMSE} < 41.9$  days).

**Table 6. MyLake performance indicators of water temperature simulations** (root mean squared error – RMSE and Pearson correlation coefficient – r) for the calibration and validation periods (val=10 years; lt-val=long-term);  $n_{\text{obs data}}$  = number of limnological observation data for comparison with simulated data.

Lake	Period	RMSE (°C)	r	$n_{\text{obs data}}$
Geneva	cal	1.143	0.961	3868
	val	1.107	0.967	3756
	lt-val	1.211	0.961	17126
Annecy	cal	1.723	0.944	1048
	val	1.952	0.938	1185
	lt-val	1.949	0.938	5231
Bourget	cal	1.022	0.963	31847
	val	1.105	0.970	6508
	lt-val	1.119	0.958	93127
Aiguebelette	cal	1.587	0.949	10901
	val	1.589	0.933	19830
	lt-val	1.608	0.941	40699

**Table 7. Comparison of model validation metrics for eight thermal indices** over 10 years and a long-term validation period (37 to 63 years) for the four lakes (see extended table in supplementary) Bold = RMSE < 2°C and  $R^2 > 0.7$ ; Italic = RMSE < 2.7°C and  $R^2 > 0.5$ .

	Lake	RMSE		$R^2$	
		10 years	*Long-term	10 years	*Long-term
Full profile - water temp	Geneva	<b>0.79</b>	<b>0.67</b>	<b>0.87</b>	<b>0.89</b>
	Annecy	<b>1.56</b>	<b>1.84</b>	<b>0.86</b>	<b>0.75</b>
	Bourget	<b>0.79</b>	<b>1.02</b>	<b>0.93</b>	<b>0.88</b>
	Aiguebelette	<b>1.48</b>	<b>1.85</b>	<b>0.86</b>	<b>0.74</b>
Epilimnion T°C	Geneva	<b>1.92</b>	2.08	<b>0.91</b>	<b>0.87</b>
	Annecy	2.02	3.69	<b>0.9</b>	0.67
	Bourget	2.01	<b>1.9</b>	<b>0.90</b>	<b>0.90</b>
	Aiguebelette	2.61	4.60	<b>0.89</b>	0.65
Hypolimnion T°C	Geneva	<b>0.68</b>	<b>0.57</b>	0.15	0.18
	Annecy	<b>0.84</b>	<b>0.9</b>	0.1	0.13
	Bourget	<b>0.51</b>	<b>0.80</b>	0.15	0.01
	Aiguebelette	<b>1.31</b>	<b>1.19</b>	0.14	0.09
Schmidt Stability (J/m <sup>2</sup> )	Geneva	3108.40	3433.10	<b>0.89</b>	<b>0.87</b>
	Annecy	820.9	5962.9	<b>0.86</b>	0.69
	Bourget	3993.60	4191.6	<b>0.89</b>	<b>0.88</b>
	Aiguebelette	1536.03	2398.21	<b>0.88</b>	0.66
Thermocline depth (m) full year / June to September	Geneva	28.00/6.3	21.20/6.39	0.27/0.14	0.22/0.12
	Annecy	11.7/7.8	11.8/8.98	0.22/0.16	0.11/0.01
	Bourget	7.92/7.11	11.5/6.91	0.69/0.25	0.37/0.23

	Aiguebelette	8.80/3.6	9.43/4.14	0.56/0.04	0.25/0.02
Stratification onset (DOY)	Geneva	32.5	20.9	0.33	0.00
	Annecy	11.4	28	0.11	0.00
	Bourget	9.4	16.7	0.33	0.17
	Aiguebelette	20.3	15.8	0.44	0.14
End-of-stratification (DOY)	Geneva	17.0	23.7	0.00	0.1
	Annecy	13.4	18.9	0.00	0.03
	Bourget	10.7	25.7	0.35	0.00
	Aiguebelette	5.45	13.2	0.7	0.18
Stratification duration (Days)	Geneva	41.9	35.4	0.00	0.14
	Annecy	26.4	31.4	0.00	0.06
	Bourget	13.1	35.4	0.12	0.04
	Aiguebelette	25.9	26.2	0.00	0.04

290

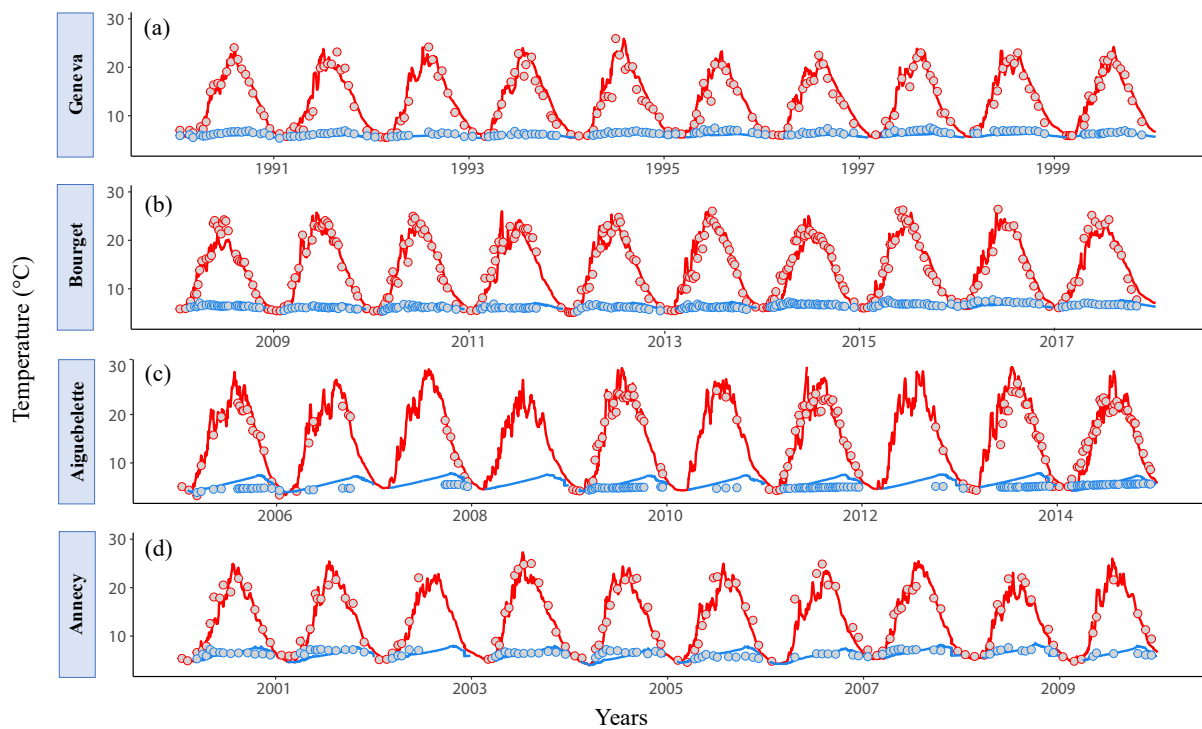
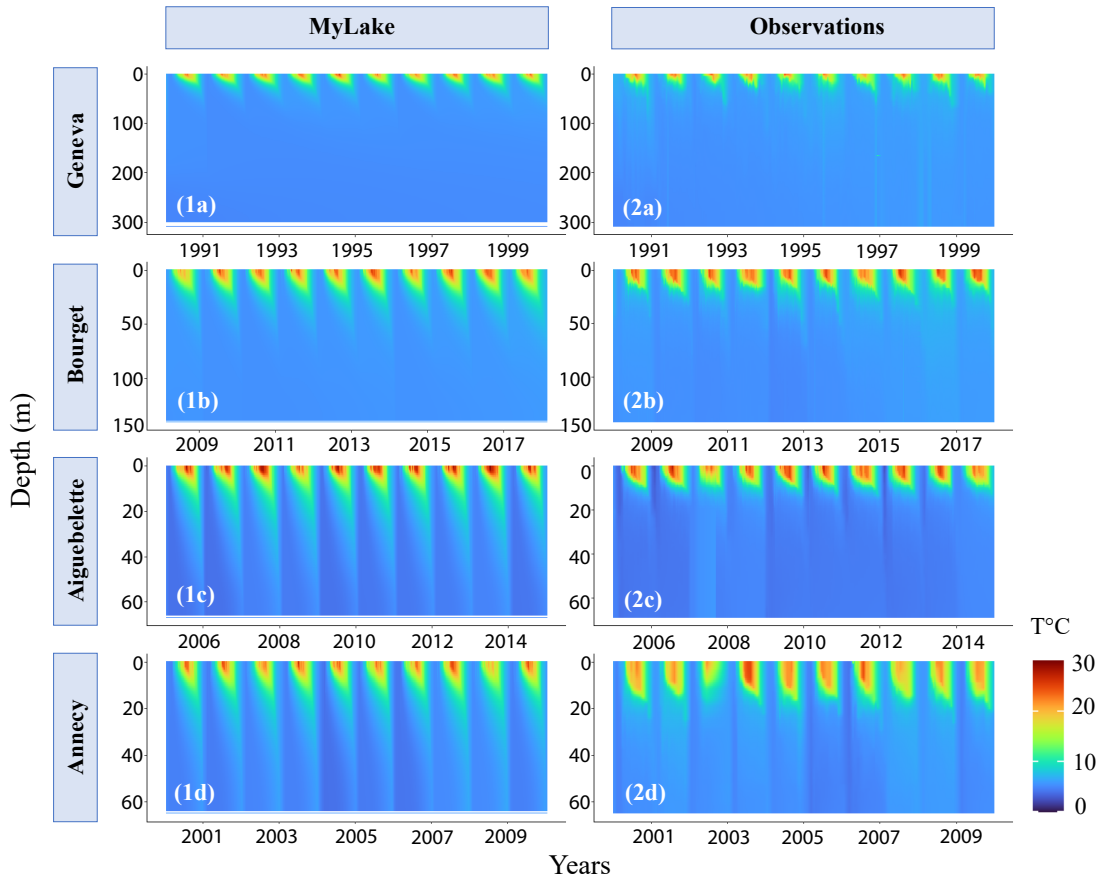


**Figure 2.** Temporal variations in epilimnion (red) and hypolimnion (blue) temperatures of Lake Geneva (a), Bourget (b), Aiguebelette (c) and Annecy (d). MyLake simulations (line) vs Observations (point) over the 10-year validation period.

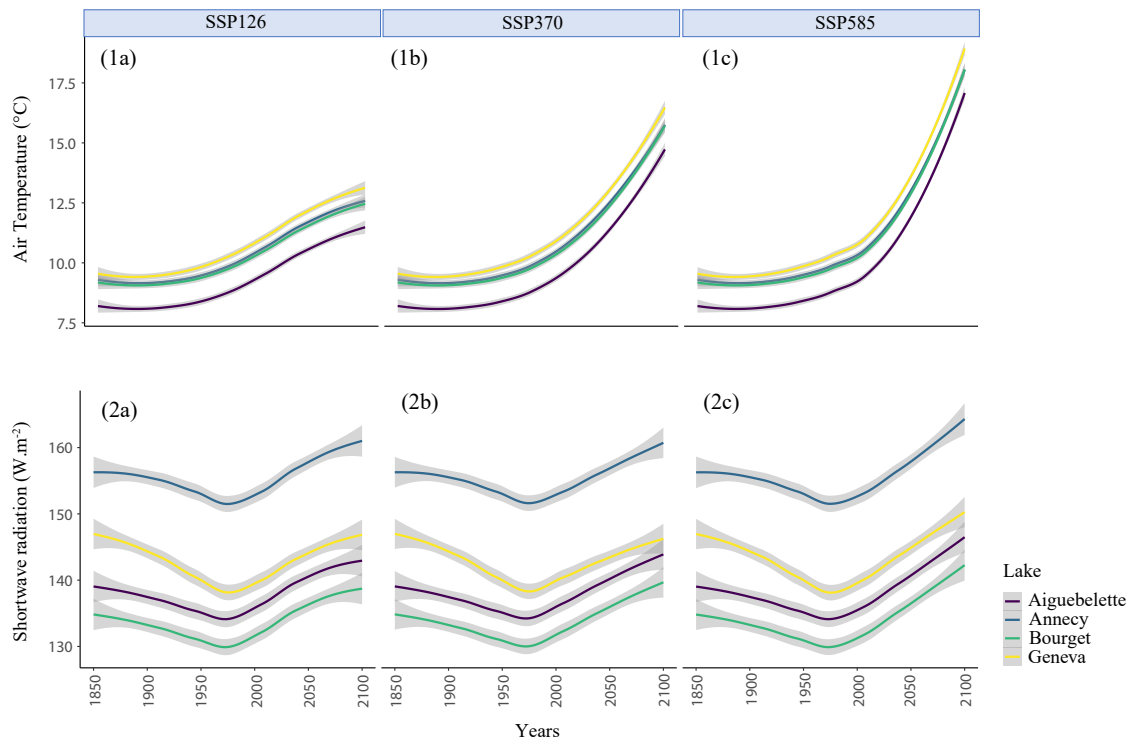




295 **Figure 3. Daily averaged MyLake water temperature simulations (1) and interpolated observations from OLA database (2) in Lake Geneva (a), Bourget (b), Aiguebelette (c) and Annecy (d) over the 10-year validation period.**

### 3.2 Meteorological trends

Based on the different scenarios adopted in the present work, mean annual air temperature has increased by +0.39 °C (Lake Bourget) and +0.5 °C (Lake Geneva) per decade over the past 30 years (from 1990 to 2020) (Fig. 4). At the horizon 2100 (from 2070 to 2100), on one hand the mean annual air temperature with the ssp126 scenario decreased on average by -0.008 °C per decade across all lakes. On the other hand, with the ssp370 and ssp585 scenarios an average increase of +0.9 °C and +1.13 °C per decade were predicted, respectively. When comparing the average annual air temperature between the two periods, increases of +1.69 °C, +4.04 °C and +5.81 °C are predicted according to ssp126, ssp370 and ssp585 scenarios, respectively. Mean annual shortwave radiations have increased on average by +1.58 W m<sup>-2</sup> per decade from 1990 to 2020 and are expected to decrease by -1.5 W m<sup>-2</sup> per decade according to the most optimistic scenario (ssp126). According to the most optimistic scenario (ssp126), an increase of +6.21 W m<sup>-2</sup> is expected at the horizon 2100, unlike the most pessimistic scenario (ssp585) that predicted an increase of +7.66 W m<sup>-2</sup>.



310

**Figure 4. Selected meteorological forcing variables over studied period 1850-2100.** Projected evolution of air temperature (1) and shortwave radiation (2) from IPSL-CM6A-LR (ISIMIP3b) under ssp126 (a), ssp370 (b) and ssp585 (c) for the four lakes (Geneva, Anney, Bourget, Aiguebelette), from 1850 to 2100 (statistical method = loess).

### 315 3.3 Lakes response to the meteorological scenarios

#### 3.3.1 Water temperature

The epilimnion temperature increased by around  $0.44\text{ }^{\circ}\text{C decade}^{-1}$  (Lake Aiguebelette) to  $0.48\text{ }^{\circ}\text{C decade}^{-1}$  (Lake Geneva) over the past 30 years (1990-2020). In the future projections (2070-2100), according to the most optimistic scenario (ssp126), a decrease of  $-0.07$  to  $-0.08\text{ }^{\circ}\text{C decade}^{-1}$  could be expected (Fig. 5). The intermediate scenario (ssp370) predicted a significant increase of  $+0.77\text{ }^{\circ}\text{C decade}^{-1}$  (Lake Anney) to  $+0.89\text{ }^{\circ}\text{C decade}^{-1}$  (Lake Geneva). In the worst-case scenario, the epilimnion temperature in the four lakes could increase by  $+1.03\text{ }^{\circ}\text{C decade}^{-1}$  (Lake Anney) to  $+1.13\text{ }^{\circ}\text{C decade}^{-1}$  (Lake Geneva). In all cases, a significant change in epilimnion temperature was predicted by the model over the two periods.

Over the last 30 years, hypolimnion temperature increased by  $+0.29\text{ }^{\circ}\text{C}$ ,  $+0.31\text{ }^{\circ}\text{C}$ ,  $+0.32\text{ }^{\circ}\text{C}$  and  $+0.39\text{ }^{\circ}\text{C decade}^{-1}$  in Lake Aiguebelette, Geneva, Anney, and Bourget, respectively. The rate of increase was higher for surface layers than for deep hypolimnetic layers. The difference between the epilimnion and hypolimnion warming rates was larger for Lake Geneva. A less significant increase in hypolimnion temperature could be expected at the horizon 2100 according to the ssp126 scenario, with  $+0.19\text{ }^{\circ}\text{C decade}^{-1}$  (Lake Geneva) to  $+0.3\text{ }^{\circ}\text{C decade}^{-1}$  (Lake Bourget). Unlike the epilimnion, even the most optimistic scenario predicted an increase in deep layers. In the four lakes, a significant rise in  $+0.55\text{ }^{\circ}\text{C decade}^{-1}$  (Lake Anney) to  $+0.73\text{ }^{\circ}\text{C decade}^{-1}$  (Lake Bourget) was expected in the case of the intermediate scenario. The ssp585 scenario predicted an increase by  $+0.67\text{ }^{\circ}\text{C decade}^{-1}$  (Lake Anney) to  $+0.82\text{ }^{\circ}\text{C decade}^{-1}$  (Lake Geneva).

325  
330

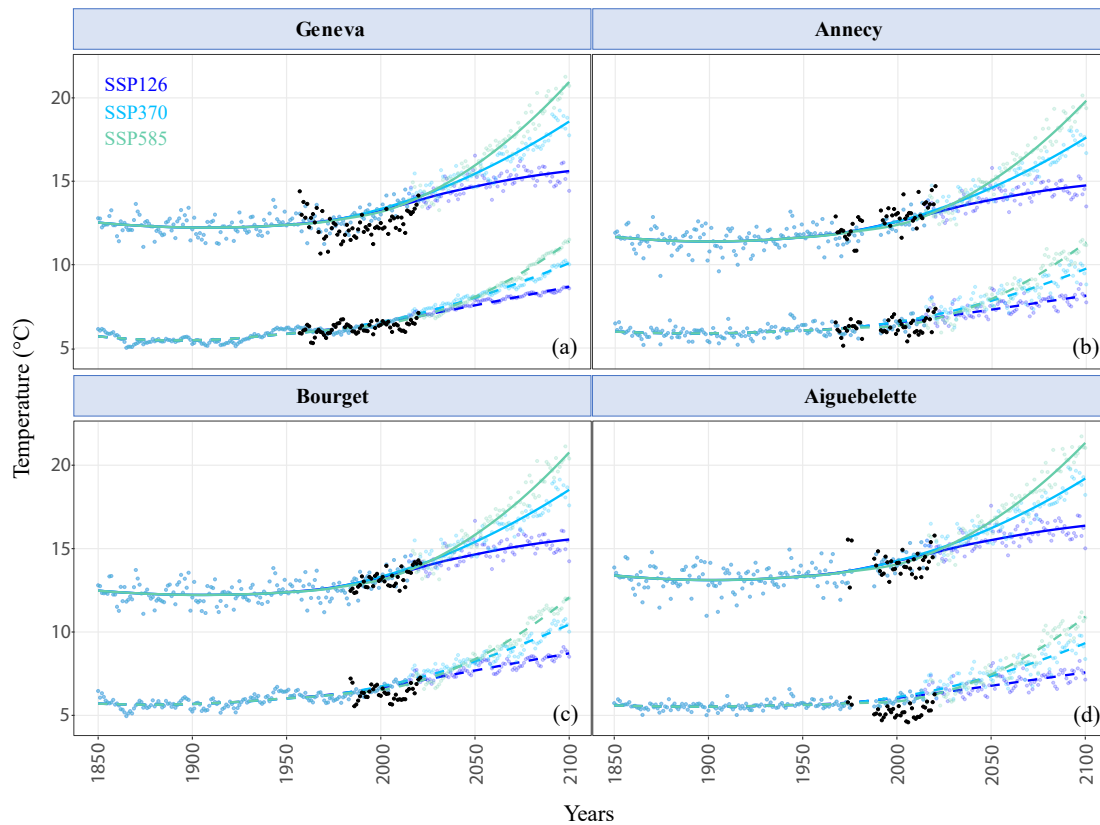
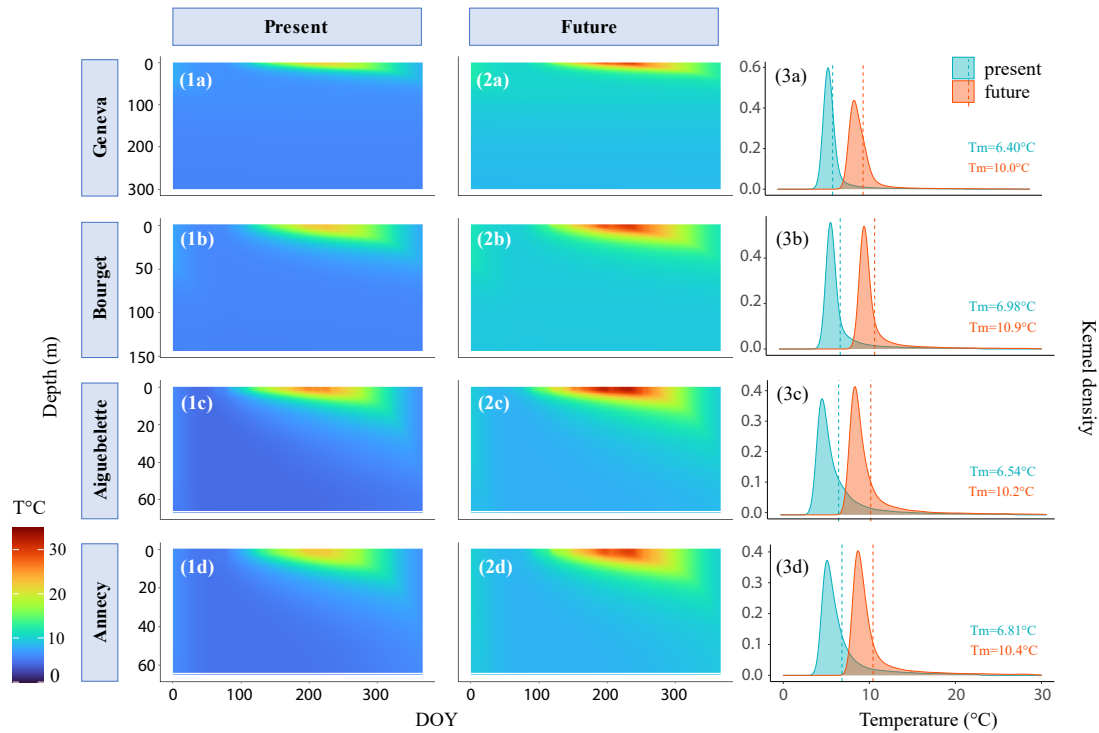


**Figure 5. Annual averages of epilimnion (line) and hypolimnion (dashed lines) temperatures** from MyLake daily water temperature simulations over the period 1850-2100, for three different climate scenarios (ssp126, ssp370, ssp585) in Lake Geneva (a), Annecy (b), Bourget (c), and Aiguebelette (d). Black dots represent annual averages of observation data.

The water temperature change was quantified as the non-overlapped area of the two daily averaged temperature distributions in the present (2000-2010) and the future (2090-2100) as a percentage of the combined area of those distributions for the intermediate scenario (ssp370) (Fig. 6). The greatest thermal change occurred in Lake Geneva and Bourget with 90 % and 86 % non-overlap respectively between the two periods. In Lake Annecy and Aiguebelette, 77 % and 76 % thermal non-overlap were predicted, respectively.

The annual average temperature was expected to increase between the two periods on average by +3.59, +3.60, +3.66 and +3.92 °C in Lake Annecy, Geneva, Aiguebelette and Bourget respectively.





345 **Figure 6. MyLake water temperature simulations** from intermediate climate scenario (ssp370). Daily averaged water temperature over the periods 2000-2010 (1) and 2090-2100 (2) in Lake Geneva (a), Bourget (b), Aiguebelette (c), and Annecy (d). Estimated frequency of daily average temperature data (3) over these present (2000-2010) and the future (2090-2100) using kernel density. The dashed lines represent average annual temperatures over the entire periods.

### 3.3.2 Stratification characteristics

350 Schmidt stability, describing the stability of the water column and its resistance to mixing, has significantly increased over the past 30 years by an annual average of  $+174.6 \text{ J m}^{-2} \text{ decade}^{-1}$ ,  $+522.97 \text{ J m}^{-2} \text{ decade}^{-1}$ ,  $+654,57 \text{ J m}^{-2} \text{ decade}^{-1}$ , and  $+1753.5 \text{ J m}^{-2} \text{ decade}^{-1}$  for Lake Annecy, Aiguebelette, Bourget and Geneva respectively (Fig. 7). No significant trend was predicted by the model at the horizon 2100 for the ssp126 scenario in Lake Geneva and Bourget. For Lake Annecy and Aiguebelette, a significant decrease of  $-100.5 \text{ J m}^{-2} \text{ decade}^{-1}$  and  $-281.3 \text{ J m}^{-2} \text{ decade}^{-1}$  could be expected according to that  
 355 optimistic scenario, respectively. The evolutions predicted by the model in the case of the intermediate scenario varied between the four lakes, with an increase of  $+285.5 \text{ J m}^{-2} \text{ decade}^{-1}$  in Lake Annecy,  $+927.8 \text{ J m}^{-2} \text{ decade}^{-1}$  in Aiguebelette,  $+1088.7 \text{ J m}^{-2} \text{ decade}^{-1}$  in Bourget, and  $+3435 \text{ J m}^{-2} \text{ decade}^{-1}$  in Lake Geneva. In the worst-case scenario (ssp585), an increase of  $+445 \text{ J m}^{-2} \text{ decade}^{-1}$  (Lake Annecy) to  $+4695 \text{ J m}^{-2} \text{ decade}^{-1}$  (Lake Geneva) could be expected. For the four lakes, in any scenario, a significant evolution was predicted by the model between the last 30 years and the future (2070-2100), however with different  
 360 annual averages from one lake to another (Schmidt stability= $2646 \text{ J m}^{-2}$  and  $23042 \text{ J m}^{-2}$  for Lake Annecy and Geneva respectively).

No significant trend was identified for the day of onset of stratification (DOY) in the present and the future, except for Lake Annecy according to ssp126 scenario (DOY =  $+1.6 \text{ days decade}^{-1}$  and  $+4.3 \text{ days decade}^{-1}$  for present and future periods respectively) (Fig. 7). For Lake Geneva, the onset of stratification occurred significantly earlier in the case of ssp585 by on average 11 days on average (DOY=96 and 85 in the present and the future respectively), contrary to the ssp126 scenario, which predicted a significant delay of 5 days later (DOY=96 to 101 for present and future periods respectively). No significant change in stratification onset has been identified for Lake Annecy, Bourget and Aiguebelette. **When comparing the average days of stratification onset between the last 30 years and at the horizon 2100, a significant difference appeared only for Lake**

Geneva according to ssp126 and ssp585 scenarios. Indeed, a 6 days delay was predicted by the model in the most optimistic scenario against a 11 days advance in the most pessimistic scenario.

In regards to the break-up of stratification, a significant trend was only predicted for Lake Geneva in the present (1990-2020) with an average of 5 days decade<sup>-1</sup> later. Except for Lake Annecy and Aiguebelette ssp126 and Lake Bourget ssp370, the end of stratification appeared significantly later in the future than in the last 30 years. In the ssp126 scenario, the stratification could end on average 6 days and 5 days earlier for Lake Geneva and Bourget, respectively. According to the ssp370 scenario, it was predicted to end on average 5.7 days, 7.4 days and 3 days later in Lake Annecy, Geneva and Aiguebelette, respectively. In the worst-case scenario, a delay of 7.7 days, 14.7 days, 6.8 days and 3.6 days in Lake Annecy, Geneva, Bourget and Aiguebelette, respectively.

As a result, a significant increase in the average stratification duration was predicted in Lake Geneva – ssp585 of +21.2 days (DOY<sub>present</sub>=278.3 and DOY<sub>future</sub>=299.5). In the most optimistic scenario (ssp126), a significant decrease could be expected in Lake Geneva and Bourget (-8.8 days and -9.45 days, respectively) between the two periods. No significant difference was predicted by the model for Lake Annecy and Aiguebelette. The average duration of stratification within the four lakes was from 246 days (Lake Annecy) to 279 days (Lake Geneva) for the present period. In the worst-case scenario, the duration could last from 251 days (Lake Annecy) to 300 days (Lake Geneva).

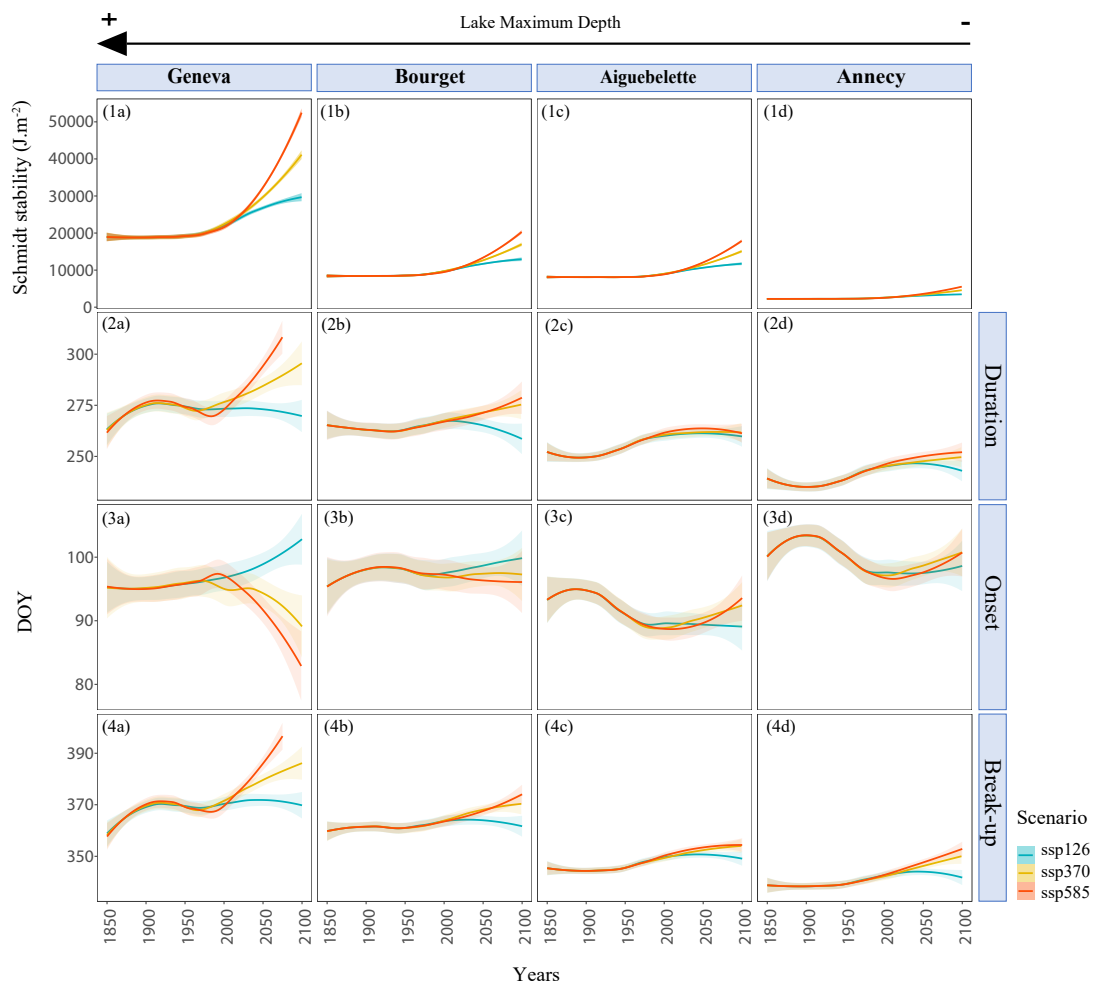


**Figure 7. Stratification trend characteristics for the four lakes (Geneva (a), Bourget (b), Aiguebelette (c) and Annecy (d)).** Estimations of Schmidt stability (1) from June to September, stratification duration (2), onset (3), and break-up (4) over the period 1850-2100 for the 3 scenarios (ssp126, ssp370, and ssp585), calculated from MyLake water temperature simulations.

### 3.3.3 Water volumes: habitat

390 Changes in thermal habitat between the present (2000-2010) and the future (2090-2100) were assessed based on the  
lake volume fraction that exceeded specific temperature thresholds ( $>7\text{ }^{\circ}\text{C}$ ,  $>9\text{ }^{\circ}\text{C}$ , and  $>12\text{ }^{\circ}\text{C}$ ) (Fig. 8), above which the  
reproduction, growth, and survival of certain fish species may be affected (Mari et al., 2016b; Réalis-Doyelle, 2016). These  
lake volume fractions were calculated from daily average water temperature simulated by MyLake model and the bathymetry  
file. Annual averages have been calculated from these daily data and were then quantified as the non-overlapped area of the  
395 two lake volume fraction distributions (present and future based on the 3 different scenarios). Kernel density allowed to  
compare both lake volume fractions but also the number of days associated to them. In Lakes Geneva and Bourget, temperature  
was predicted to exceed  $7\text{ }^{\circ}\text{C}$  in all case scenarios, with a lake volume fraction non-overlap of 100 % between the present  
(2000-2010) and the future (2090-2100). In Lake Annecy, 77.8 % of the water column could reach a temperature greater than  
 $7\text{ }^{\circ}\text{C}$  in the ssp126 case-scenario and could extend to the entire water column in the two other scenarios, with a 100 % non-  
400 overlap between present and future projections. In Lake Aiguebelette, the lake volume fraction with temperature above  $7\text{ }^{\circ}\text{C}$   
has increased from 15 % (present) to 87 % (ssp370 and ssp585), involving a lake volume fraction non-overlap of 49 % (ssp126)  
and 100 % (ssp370 and ssp585). In all lakes, a significant increase of water volume above  $7\text{ }^{\circ}\text{C}$  was predicted by the model  
for the three scenarios.

In Lake Annecy, Geneva, and Bourget, temperature could exceed  $9\text{ }^{\circ}\text{C}$  according to the intermediate scenario (annual  
405 average lake volume fraction=70 %, 84 %, and 100 % respectively). According to the ssp585 scenario, temperatures of almost  
the entire lakes could reach  $9\text{ }^{\circ}\text{C}$  (annual average lake volume fraction=96-100 %). The specific bathymetry of Lake  
Aiguebelette caused a progressive increase of lake volume fraction with temperature above  $9\text{ }^{\circ}\text{C}$ , yet never reached the total  
volume (72.5 % of the lake for ssp585). According to the ssp126 scenario, lake volume fraction with temperature above  $9\text{ }^{\circ}\text{C}$   
non-overlap was 35 %, 47 %, 61 %, and 62 % for Lake Aiguebelette, Annecy, Bourget and Geneva respectively. The increase  
410 was more important for the two larger and deeper lakes. In all cases, the model predicted a significant change between present  
and the three future scenarios. The thermal overlaps between the present and the future according to ssp585 scenarios were  
predicted to reach 100 % for all four lakes. This means that the average daily lake volume fraction with temperature above  $9\text{ }^{\circ}\text{C}$   
was expected to be completely different between the two periods, with higher values in the future. A 100 % increase was  
also predicted in the ssp370 case-scenario for Lake Geneva and Bourget, against 69 % and 75 % for Lakes Aiguebelette and  
415 Annecy, respectively.

Water volumes above  $12\text{ }^{\circ}\text{C}$  have increased by on average by +45 % (ssp126) for Lakes Annecy, Geneva, and  
Bourget, with a slightly smaller increase in Lake Aiguebelette (+30 % of lake volume fraction non-overlapped). The model  
predicted the same increase in the ssp370 case scenario for the two deepest lakes (Geneva and Bourget) with on average +70  
% of lake volume fraction non-overlap. In Lake Aiguebelette and Annecy, +53 % and +34 % could be expected, respectively.  
420 Finally, in the worst-case scenario (ssp585), a higher increase in water volume above  $12\text{ }^{\circ}\text{C}$  was predicted for Lake Geneva  
(+91 % of non-overlap), followed by Lake Bourget (+82 % of non-overlap), Lake Annecy (+70 % of non-overlap) and Lake  
Aiguebelette (+64 % of thermal non-overlap).

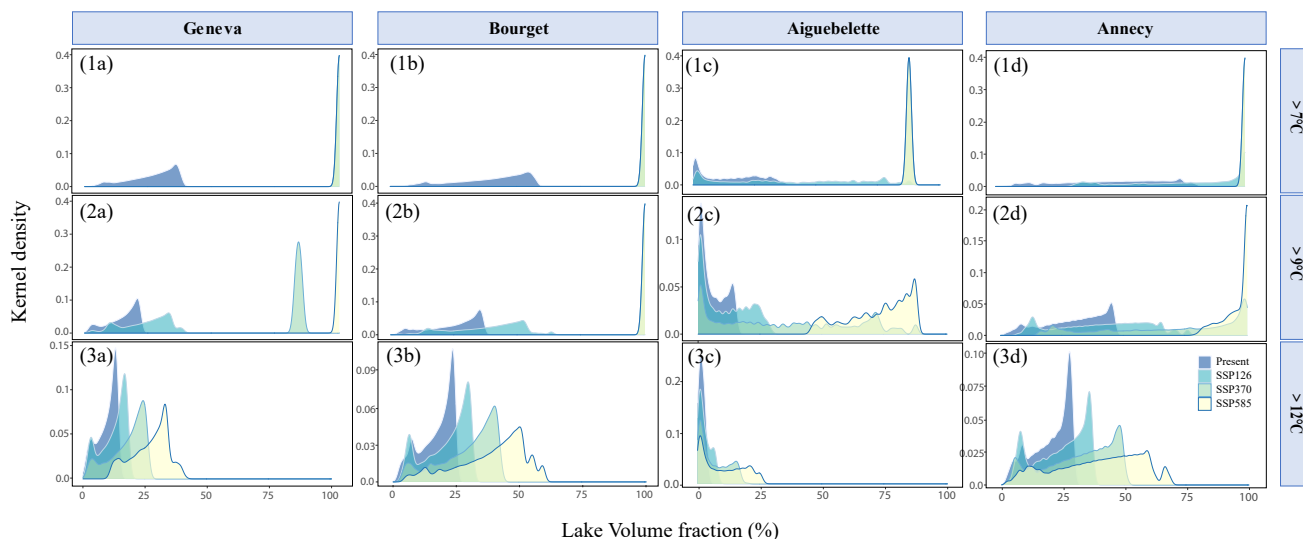
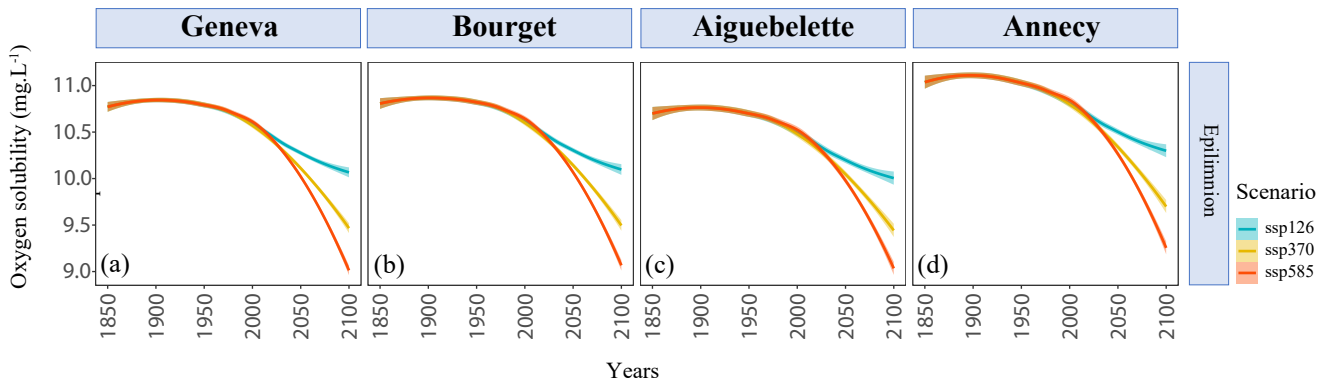


**Figure 8. Lake volume fraction with temperature exceeding three characteristics thresholds (7 °C (1), 9 °C (2), and 12 °C (3)) calculated from simulated water temperature profile and bathymetry in Lake Geneva (a), Bourget (b), Aiguebelette (c), and Annecy (d). Kernel density estimates of daily average lake volume fraction over the present (2000-2010) and the future (2090-2100) predicted by the three scenarios (ssp126, ssp370 and ssp585).**

### 3.3.4 Oxygen solubility

Oxygen solubility was calculated from the Winkler tables, as a function of temperature. In all scenarios, significant trends in potential oxygen solubility were predicted by the model for the four lakes. Over the last 30 years (1990-2020), an average annual decrease of -0.07, -0.09, -0.12, and -0.13 mg L<sup>-1</sup> decade<sup>-1</sup> was computed for Lake Geneva, Aiguebelette, Annecy, and Bourget, respectively (Fig. 9). At the horizon 2100 (2070-2100), according to the ssp126 scenario, a decrease of -0.05 mg L<sup>-1</sup> decade<sup>-1</sup> (Lakes Geneva and Aiguebelette) to -0.09 mg L<sup>-1</sup> decade<sup>-1</sup> (Lake Bourget) could be expected. A significant decrease of -0.16 mg L<sup>-1</sup> decade<sup>-1</sup> (Lake Geneva) to -0.21 mg L<sup>-1</sup> decade<sup>-1</sup> (Lakes Bourget and Aiguebelette) was predicted in the intermediate scenario and from -0.17 mg L<sup>-1</sup> decade<sup>-1</sup> (Lake Annecy) to -0.23 mg L<sup>-1</sup> decade<sup>-1</sup> (Lake Bourget) in the ssp585 scenario. In all cases, a significant difference has been forecast between present and future periods within the four lakes. An annual average of 12.15, 12.21, 12.22, and 12.3 mg L<sup>-1</sup> was calculated for the present period from the model simulations in Lakes Bourget, Annecy, Geneva, and Aiguebelette, respectively. In the future predicted by the intermediate scenario, annual averages from 11.28 mg L<sup>-1</sup> (Lake Bourget) to 11.49 mg L<sup>-1</sup> (Lake Aiguebelette) could be expected.

Furthermore, the model predicted a faster decrease in oxygen solubility in the epilimnion compared to the hypolimnion in the four lakes over the last 30 years, with an average of -0.104 and -0.096 mg L<sup>-1</sup> decade<sup>-1</sup> in the epilimnion and the hypolimnion, respectively. No significant trend was forecast for oxygen solubility in the epilimnion for all lakes according to the ssp126 scenario, resulting in the stabilization of oxygen solubility. In the ssp370 case-scenario, the model predicted a decrease in oxygen solubility in the epilimnion of -0.16, -0.17 and -0.18 mg L<sup>-1</sup> decade<sup>-1</sup> in Lake Annecy, Aiguebelette and both Geneva and Bourget, respectively. According to the worst scenario (ssp585), oxygen solubility in epilimnion was expected to decrease by an average of -0.2 mg L<sup>-1</sup> decade<sup>-1</sup> ( $\pm 0.01$  mg L<sup>-1</sup> decade<sup>-1</sup>). Oxygen solubility in deep layers are expected to be closely related to its evolution into the epilimnion, depending on the intensity and depth of the water column mixing.



450

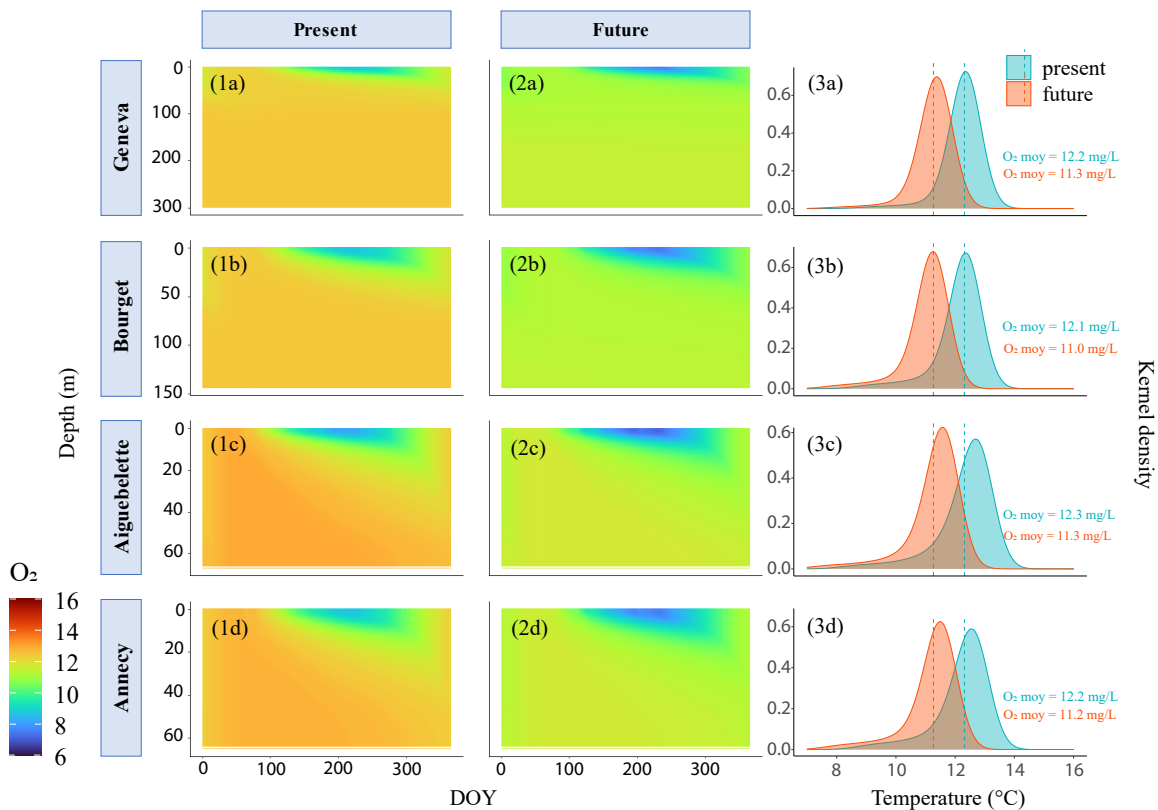
**Figure 9. Annual averages of potential oxygen solubility over the period 1850-2100, in the epilimnion calculated from MyLake daily water temperature simulations for three different climate scenarios (ssp126, ssp370, ssp585) in Lake Geneva (a), Bourget (b), Aiguebelette (c), and Annecy (d).**

455

Potential change in oxygen solubility was also quantified as the non-overlapped area of the two daily averaged oxygen solubility distributions in the present (2000-2010) and the future (2090-2100) as a percentage of the combined area of those distributions, for the intermediate scenario (ssp370) (Fig. 10). As for the thermal regime, the highest changes in oxygen solubility were in Lakes Geneva and Bourget with 60 % of non-overlap between the present and the future. In Lakes Aiguebelette and Annecy, the non-overlap rate has been reduced to 55 % and 54 %.

460

Annual potential average oxygen solubility was predicted to decrease by  $-0.9 \text{ mg L}^{-1}$  (Lake Geneva) to  $-1.1 \text{ mg L}^{-1}$  (Lake Bourget) in the future.



465

**Figure 10. Potential oxygen solubility in lake waters of the four lakes, calculated from MyLake water temperature simulations for the intermediate climate scenario (ssp370). Daily averaged oxygen solubility over the present (1) and future (2) in Lakes Geneva (a), Bourget (b), Aiguebelette (c), and Annecy (d). Estimated frequency of daily average oxygen solubility (3) over the present (2000-2010) and future (2090-2100) using kernel density. The dashed lines represent annual average oxygen solubility over the entire periods.**



As for the thermal habitat, water volumes with sufficient dissolved oxygen levels to support fish survival were assessed based on lake volume fraction that exceeded certain thresholds (10 mg L<sup>-1</sup> and 11 mg L<sup>-1</sup>) (Fig. 11). The differences between the present (2000-2010) and the future (2090-2100) according to the three scenarios were then quantified as the non-overlapped area of the two lake volume fraction distributions. Kernel density allowed to compare the evolution of potential oxygen solubility over a full year, between present and future. The non-overlap areas quantification between these two periods was a good way to represent both the difference in potential oxygen solubility and the number of days associated, during one year. In the present, an average of 95.6 % (±1.6 %) of the total lake volume had a potential oxygen solubility >10 mg L<sup>-1</sup> in Lakes Annecy, Geneva, and Bourget, unlike Lake Aiguebelette with only 61.2 % of the lake volume. Averages of 25.8 % (±3.2 %), 40.5 % (±3.5 %) and 48.3 % (±5.3 %) of lake volume fraction non-overlap was predicted in ssp126, ssp370 and ssp585 scenarios, respectively. In the worst-case scenario, lake volume fractions were expected to be reduced to 85.9 %, 92 %, 86.8 % and 57.7 % for Lakes Annecy, Geneva, Bourget and Aiguebelette respectively.

In the two deepest lakes (Geneva and Bourget), the lake volume fraction with potential oxygen solubility above 11 mg L<sup>-1</sup> has decreased gradually according to the 3 scenarios, and reached 100 % of non-overlap between the present and the future (ssp585). The decrease was less sharply for Lakes Annecy and Aiguebelette, with 72 % and 68 % of non-overlap in ssp585 scenario, respectively. Although, in the intermediate scenario, 68.7 % (Geneva), 67.7 % (Annecy), 61.6 % (Bourget), and 48.6 % (Aiguebelette) of the total lake volume could have potential dissolved oxygen levels greater than 11 mg L<sup>-1</sup>. These lake volume fractions could be reduced to 52.3 %, 41.3 %, 33.2 %, and 26.8 % in Lakes Annecy, Aiguebelette, Geneva, and Bourget respectively, in the worst-case scenario.

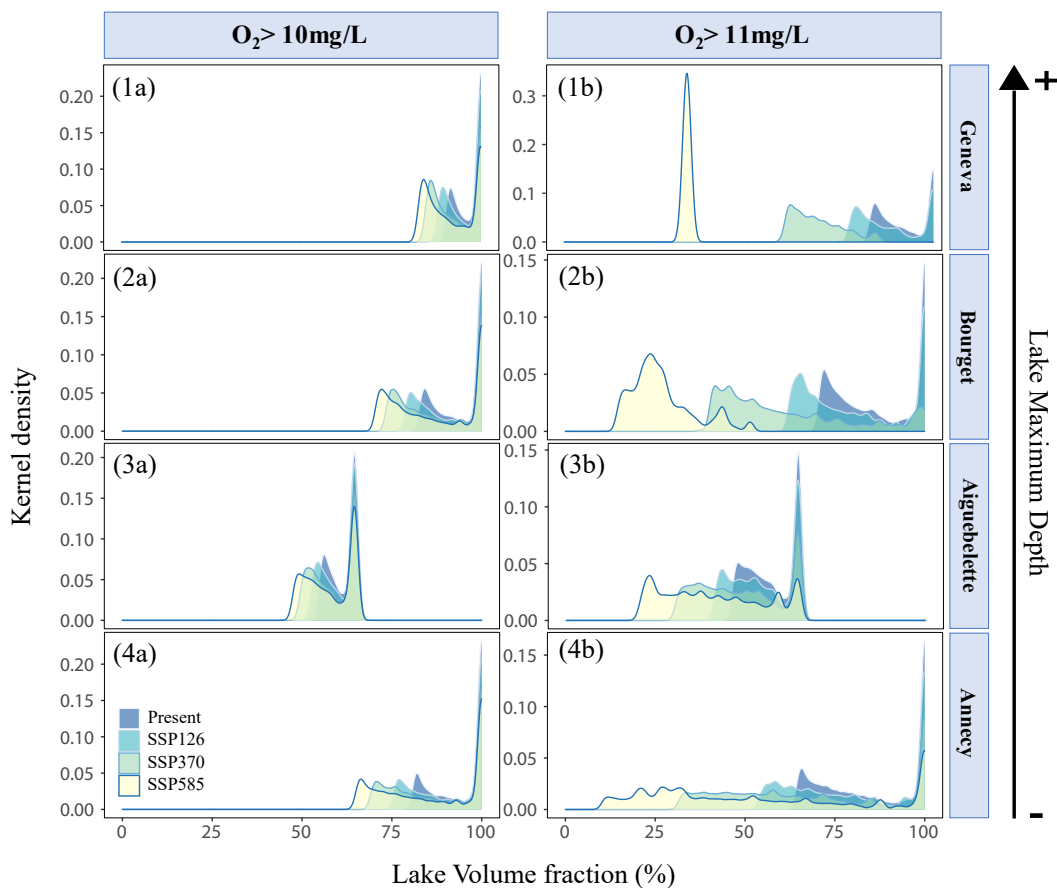


**Figure 11. Lake volume fraction with oxygen solubility exceeding two thresholds (10 (1) and 11 mg L<sup>-1</sup> (2)), calculated from simulated water temperature profiles and bathymetry in Lake Geneva (a), Bourget (b), Aiguebelette (c) and Annecy (d). Kernel density estimates of daily average lake volume fraction over the present (2000-2010) and the future (2090-2100) predicted by the three scenarios (ssp126, ssp370 and ssp585).**

## 4. Discussion

### 4.1 Large perialpine lakes warming

495 Most lakes in the world tend to warm due to climate change, with a mean increase of  $+0.34\text{ }^{\circ}\text{C decade}^{-1}$  in their surface water temperatures during summer between 1985 and 2009 (O'Reilly et al., 2015). Our study shows that large perialpine lakes tend to warm at fast rates, with mean epilimnetic temperature increase of  $+0.46\text{ }^{\circ}\text{C decade}^{-1}$  in the case of Lakes Geneva, Bourget, Aiguebelette and Annecy. These rates of change in surface water temperature are congruent with those found for other perialpine lakes over the period 1975-2015 (Ficker et al., 2017). Moreover, it is consistent with the average increase in air temperature (from 0.39 to 0.5  $^{\circ}\text{C per decade}$ ), indicating a direct response in lake temperature trends, as expected. The epilimnion of our studied lakes experienced higher warming rates than in the hypolimnion. This observation is in accordance with the expected increasing density gradients, leading to a deeper stratification which isolates deep layers from wind energy, reduces vertical mixing and prevent hypolimnetic water temperatures from increasing (Fernández Castro et al., 2021). Further, in deep lakes, the dynamic of deep-water temperature is linked with the extend and frequency of total winter mixing (Dokulik et al., 2001) and inter-total mixing periods, characterized by regular increase in deep water temperature.

In the future, simulated water temperatures showed different responses to global warming under different projections. In the most optimistic scenario, where strong environmental and political measures would be implemented, surface water temperatures are expected to decrease, whereas hypolimnetic water are expected to warm. The mechanistic effect of surface cooling in the most optimistic scenario over 1970–2100 is explained by the future development of both air temperature and solar radiation predicted to decrease. The recent past trend of surface warming is not expected to persist in the future in other large deep lakes in Central Europe (Schmid and Köster, 2016). Despite that, hypolimnion warming could be explained by the thermal inertia and heat accumulation in deep waters (Crossman et al., 2016). In the intermediate (ssp370) and most pessimistic (ssp585) scenarios, both epilimnion and hypolimnion temperatures are increasing driven by higher rates of air temperature warming in comparison to the recent past warming, with higher increases in the two deepest lakes (Geneva and Bourget) and faster warmings of the surface layers than deep layers. Similarly, the entire water column of the two shallowest lakes (Annecy and Aiguebelette) could warm up less quickly than the two deepest ones. This might be explained by less frequent complete mixing in deeper lakes, leading to longer inter-mixing periods during which water temperature increases. However, by 2100, there is a high probability that the hydrological regime in the Rhône River upstream Lake Geneva changes because of an earlier snow melting leading to an earlier, and maybe shorter, input of cold water into the lake. The effects of hydrological changes on the thermal regime of large deep lakes are expected to be relatively modest, such as observed in preliminary sensitivity tests (results not shown here). However, these interactions would require further investigations, especially in the case of lakes supplied by upstream snow and glacier area.

### 4.2 Implications on oxy-thermal habitats

525 Dissolved oxygen is one of the most fundamental variable in lake systems (Wetzel, 2001b). Dissolved oxygen depends on several variables, such as oxygen solubility and hydro-meteorological conditions (Rajwa-Kuligiewicz et al., 2014), but also the intensity of biological processes such as photosynthesis, respiration and decomposition of organic matter.

Jane et al., (2021) found that a decline in dissolved oxygen is widespread in surface water habitats, primarily associated with reduced solubility under warmer water temperatures. Here, we investigate changes in oxygen solubility, i.e. the oxygen concentration in solution in equilibrium with the oxygen pressure in a gas phase, as function of temperature.

In the four perialpine lakes, oxygen solubility as a function of water temperature has decreased in both surface and deep waters over the last 30 years, with differences in amplitude. Water warming explained average rates of changes of  $-0.1\text{ mg L}^{-1}\text{ decade}^{-1}$  in oxygen solubility over that period, which are similar to those observed in temperate lakes (Jane et al.,

535 2021). Lake Geneva and Bourget would face the greatest decrease in oxygen solubility, which is consistent with previous observations on thermal changes. Moreover, a faster decrease in the epilimnion has been identified, which was correlated to a higher increase in the water temperature of surface layers and did not consider the negative effect of shorter and less deep mixing periods on DO in hypolimnion.

540 Despite the decrease in oxygen solubility being a direct inference of the increase in water temperature, our approach allows us to quantitatively assess oxy-thermal habitat changes in a global warming context relative to the long-term evolution of the water temperature. Our analysis provides a broader context for climate change impacts on lakes physics that goes further than water warming, but also have implications in terms of oxy-thermal habitat changes that may increase the likelihood of community disruptions due to the disappearance of habitat over their suitable thermal ranges (Kraemer et al., 2021). However they do not integrate oxygen consumption and production by photosynthesis, or lateral flow paths and production in littoral zones which can be important for large and deep lake ecosystems. It would need to be adjusted with studies dealing ecosystem oxygen production and consumption in the pelagic zone.

550 Finally, the effect of decreased oxygen solubility on fish habitats was assessed through some potential thresholds. The model predicted faster decreases of the lake volume fraction with oxygen solubility  $>11 \text{ mg L}^{-1}$  in the two deepest lakes (Geneva and Bourget), according to the three scenarios. For instance, the decrease in oxygen solubility can reduce habitat for cold water fish, who could face warmer water temperature and lower dissolved oxygen concentrations (Mohseni et al., 2003).

### 4.3 Sensitivity of peri-alpine lakes to climate change

555 The four perialpine lakes share the same climate region and, as a result of their large size they also share the same topographical properties to varying extent. Despite similarities, the four studied lakes tend to respond differently to climate change. For instance, the highest increase of Schmidt stability was predicted in Lake Geneva according to ssp370 and ssp585 scenarios, Lake Annecy being the least sensitive. These results seemed to be consistent as changes in stability vary by lake archetype, with larger increases in deeper and more turbid lakes (Butcher et al., 2015). Regardless of the climate scenario, an increase in the stratification intensity and duration with depth is expected in the four lakes. Accordingly, Lake Geneva was predicted to experience the highest changes in the start, end and duration of stratification, with a significant advance in stratification onset, later end-of-stratification and longer stratification duration. This is consistent with its greater resistance to mixing, but it has also the particularity to mix over the whole water column in particular years under specific meteorological conditions (last full mixing of its water column in 2012). Thus, Lake Geneva must be sensitive to the frequency of the complete water column mixing, that should be investigated more in detail in upcoming studies. Conversely, the shallowest lake (Annecy) was predicted to stratified the latest with the shortest duration in all scenarios. This analysis showed that in future projections, Lake Geneva will be more vulnerable to global warming than Lake Annecy, with a depth-related vulnerability gradient. These results are coherent with the differential warming of surface and deep waters, which could influence the strength and duration of a lake's stratification period (Råman Vinnå et al., 2021). Finally, in the four lakes, the stratification duration should last longer with an early spring and a gradual delay of cold temperatures in autumn. The changes in the beginning, end and duration of stratification could also have an impact on oxygenation conditions in deep waters (Roberts et al., 2009b), in addition to the oxygen solubility decreasing when water temperature increases. But all these results should be considered with caution as the wind exposure is very different within the four lakes (with greater exposure for Lake Geneva) and could counteract the increase in thermal stratification (Butcher et al., 2015).

575 In all three scenarios, the entire water column in the four lakes would exceed  $7 \text{ }^{\circ}\text{C}$ , even in the deepest lakes such as Geneva. Likewise, the four lakes could reach a temperature above  $9 \text{ }^{\circ}\text{C}$  according to the intermediate and most pessimistic scenarios. This exceeding of temperature thresholds can impair the development and reproduction of some iconic fish species, leading to important issues for the lake managers and fishers. Previous studies have demonstrated that Arctic charr (*Salvelinus*

580 *alpinus*), an emblematic fish of perialpine Lakes (Caudron et al., 2014) has a limited thermal tolerance range compared with other salmonids (Baroudy and Elliot, 1994; Elliot and Elliot, 2010) and hatch survival decreased significantly as the water temperature at spawning increased from 5 °C to 8.5 °C (Mari et al., 2016b). In autumn, water temperature must fall below 7 °C for Arctic Charr's endocrine phenomena to occur and trigger ovulation and spermiation (Gillet et al., 2011). Similarly, female ovulation and male spermiation are completely blocked when the water temperature exceeds 10°C, and embryonic development is impacted up to total embryo mortality when the temperature exceeds 12 °C (Guillard et al., 1992). Similar deleterious effects have been observed for whitefish (*Coregonus sp.*), which requires a water temperature drop below 7 °C to stimulate the onset of spawning (Anneville et al., 2013). Furthermore, trout survival has been shown to decrease with an increase of +4 °C in water temperature (Réalis-Doyelle, 2016) and whitefish population, the main targeted fish in perialpine lakes (Anneville et al., 2017) will suffer of increased temperature (Gerdeaux, 2004 ; Eckmann, 2013).

590 Once again, the two deepest lakes (Geneva and Bourget) were the most sensitive to climate change with the most important changes in water volumes exceeding the temperature thresholds considered, especially in the worst-case scenario (ssp585). However, when focusing on the lake volume fraction exceeding these characteristic temperature thresholds, without considering the associated duration, Lake Annecy appeared to be the most sensitive with almost 75% of the lake above 12 °C in the most pessimistic scenario. The deeper the lake, the lower water volumes exceeding these temperature thresholds.

#### 4.4 Model reliability and limitations of the approach for the long term

595 The approach developed in this study, which consisted in reducing the number of forcing variables to only air temperature and shortwave radiation, was defined based on the variables with highest confidence level on the long-term predictions. This assumption is in line with the importance of both variables in warming trends in a peri-alpine lake, which were the main driving variables responding by 60 % and 40 %, respectively, of the increasing temperature trend, while all other meteorological variables showed small to negligible effects, which was assumed as representative for the majority of large deep lakes in Central Europe following a dimictic or monomictic regime (Schmid and Koster, 2016). Furthermore, it seems well adapted to long-term simulation approaches, with potential implications for paleolimnological studies, long-term forecast studies, or studies focused on the effects of climate change on lake ecological dynamics. The model errors for the long-term were relatively small for the 4 study sites, with RMSE < 2 °C during ten-year calibration and validation periods, with even better performance for the two deepest lakes (Geneva and Bourget). This could be explained by a more stable and stronger stratification in the deepest lakes with greater density gradients that would increase the model accuracy. This seems consistent as it has been shown that in deeper lakes (>40 m) GLM predicts hypolimnion temperature with greater accuracy when surface mixing dynamics have less influence on the deep layers' temperature (Bruce et al., 2018b). Further, hypolimnion temperature was indeed simulated with better precision in Lakes Geneva and Bourget in comparison to the two shallower lakes, just like epilimnion temperature and Schmidt stability. Nevertheless, the interannual variabilities were not well captured by the model. As for the thermocline depth, it was more difficult to predict by the model in Lakes Geneva, Annecy and Aiguebelette, yet good results were observed for Lake Bourget. These uncertainties could be caused in part by the presence of internal seiches, which increased the variability and made it difficult to be reproduced by 1-D models (Ayala et al., 2020).

615 Thus, applying only air temperature and downwelling shortwave radiation from climatic projections provided a well-adapted model to the study of the four perialpine lakes in the long term, even with considering only the seasonal trends in wind speed, cloud cover, air relative humidity, and rainfall. In this sense, the approach seems adequate for long-term simulation approaches. No systematic error has been identified as the model slightly underestimated (Lake Bourget) or overestimated (Lake Geneva) the water temperature, depending on the lake morphology. Positive biases could be attributed to the measurements which are carried out around mid-day and in good weather, whereas model outputs were averaged daily (Vinçon-Leite et al., 2014). Similarly, biases on estimations of the start, end and duration of stratification may be attributed to

the low frequency (i.e. bi-monthly) of limnological measurements, which do not allow precise estimations on the stratification periods. Besides this limitation, good performances for the Schmidt stability index suggest that the model could be used to assess the long-term variations in the stratification regime, while the duration still needs to be carefully interpreted.

This method allowed to overcome certain limitations such as the quality of the input files related to the climate variables scaling. For instance, the wind can be very different within a same 0.5° grid, depending on the surrounding terrain. The influence of rivers and watersheds may also be difficult to simulate on the long-term. Reducing the number of forcing variables to only air temperature and shortwave radiations is an efficient approach to analyze thermal regime and oxygen solubility trends on the long-term, as more and more studies are dedicated to forecast and explore future scenarios. However, there is a need to assess changes in the past that 1D modelling approaches could address, including hindcast and paleolimnological studies. Indeed, several applications to link paleoenvironmental data and models have been identified, such as model validation, synthesis of research findings and support of paleoecological data interpretation (Anderson et al., 2006). There is a need for models to produce physical and biogeochemical scenarios over the following years, decades and centuries (Anderson et al., 2006). Palaeoenvironmental data usually represent the only means for driving and testing simulation models in lakes where instrumental data are available only for short timescales (annual or pluri-annual).

A further limitation of this method is related to the correlation between the different climate variables, such as relative humidity and air temperature dependency. As the meteorological patterns replicated the seasonal fluctuations of each variable, this error is limited. Another possible option would have been to use weather generator to simulate climate variables evolutions, implemented to integrate these correlations.

Finally, for the four lakes, the model MyLake, based on the diffusive heat transport equations (Saloranta and Andersen, 2007b), performed best at simulating water temperature profiles, while GOTM and Flake performed the worst. The two-layer parametric representation of the evolving temperature profile or the k-ε-turbulence equations were not the most appropriate to the study sites. The GLM model, integrating the energy balance for surface mixing and the diffusive transport below thermocline (Hipsey et al., 2019), simulated with quite good precision the water temperature in Lakes Geneva and Bourget but was less performant for Lakes Annecy and Aiguebelette. Simstrat has well reproduced the temperature along the water column in Lake Geneva, quite well in Lake Bourget but was much less efficient at simulating water temperature in the two shallowest lakes, Annecy and Aiguebelette. This model, also based on the k-ε-turbulence equations (Gaudard et al., 2017), underly the assumption that the turbulent viscosity is isotropic. This might be more applicable to deeper, larger and with higher wind-exposure lakes.

## 5 Conclusion

In this study, an approach to simulate long-term trends in lake thermal regime and oxygen solubility has been tested and validated against 63 years of limnological data from the OLA lakes observatory. The approach shows that 1-D thermal lake models perform well when run only with air temperatures and shortwave radiations as forcing variables, hence allowing to overcome certain limitations related to the quality of climate input data for the long-term. Future application of the 1D model approach for long-term variations can be anticipated in the field of paleolimnology, but also to assess past and future effects of climate change on the ecological dynamics and lake habitats.

Simulations show that over the last 30 years, epilimnion temperature has increased on average by +0.46 °C decade<sup>-1</sup> in the four lakes. At the horizon 2100, simulations anticipate a minimum increase of +0.77 °C decade<sup>-1</sup> and +0.56 °C decade<sup>-1</sup> in epi- and hypolimnion respectively (Lake Annecy - ssp370) to a maximum of +1.13 °C decade<sup>-1</sup> (epilimnion) and +0.82 °C decade<sup>-1</sup> (hypolimnion) (Lake Geneva – ssp585). The response to climate change varies between lakes, with the deepest lakes (Bourget and Geneva) experiencing the fastest warming, with on average +3.92 °C and +3.6 °C at the horizon 2100.



In regards to oxygen condition, a decrease in oxygen solubility occurred over the last 30 years at least in Lakes Annecy and Bourget, with  $-0.12 \text{ mg L}^{-1}$  and  $-0.13 \text{ mg L}^{-1} \text{ decade}^{-1}$  respectively. At the horizon 2100, simulations indicate that Lakes Bourget and Geneva will face the greatest decrease of oxygen solubility, with  $-0.21 \text{ mg L}^{-1} \text{ decade}^{-1}$  according to the intermediate scenario, which may alter the chemical and ecological functioning of the lakes. Simulations of the duration and intensity of thermal stratification suggest that the decrease in lake oxygen conditions will be more pronounced in the case of Lake Geneva and that Lake Annecy would be the least sensitive to climate change.

#### 670 **Code and data availability**

Code and data used in this paper are available from the corresponding author upon a reasonable request.

#### **Author contributions**

675 JPJ, OD, DB, PAD, BVL conceived and designed the study. OD performed the analyses, calculation and wrote the original draft of the paper. JPJ supervised the manuscript from the methodological and long-term trend analysis perspectives. All authors actively took part in the interpretation of the results and revisions of the paper.

#### **Competing interests**

The contact author has declared that neither they nor their co-author has any competing interests.

680

#### **Disclaimer**

#### **Acknowledgements**

685 We thank the HESS editor, the reviewers and the participants of the lively discussion in HESSD for their comments that helped to improve the paper. We gratefully acknowledge the financial support from the ANR C-ARCHIVES and the Pole ECLA (French Research Organization in Lake Ecology). We would like to thank the French Observatory of Lakes (OLA) for providing the long-term limnological data and Victor Frossard from CARRTEL for thorough advances on the manuscript conception.

690

#### **Financial support**

This research has been supported by the ANR C-ARCHIVES (grant no. 5283) and the Pole ECLA.

#### **Review statement**

695

## References

- Anderson, N. J., Bugmann, H., Dearing, J. A., and Gaillard, M.-J.: Linking palaeoenvironmental data and models to understand the past and to predict the future, *Trends Ecol. Evol.*, 21, 696–704, <https://doi.org/10.1016/j.tree.2006.09.005>, 2006.
- 700 Anneville, O., Beniston, M., Gallina, N., Gillet, C., Jacquet, S., and Lazzarotto, J.: L’empreinte du changement climatique sur le Léman, *Arch. Sci.*, 16, 2013.
- Ayala, A. I., Moras, S., and Pierson, D. C.: Simulations of future changes in thermal structure of Lake Erken: proof of concept for ISIMIP2b lake sector local simulation strategy, *Hydrol. Earth Syst. Sci.*, 24, 3311–3330, <https://doi.org/10.5194/hess-24-3311-2020>, 2020.
- 705 Balsamo, G., Salgado, R., Dutra, E., Boussetta, S., Stockdale, T., and Potes, M.: On the contribution of lakes in predicting near-surface temperature in a global weather forecasting model, *Tellus Dyn. Meteorol. Oceanogr.*, 64, 15829, <https://doi.org/10.3402/tellusa.v64i0.15829>, 2012.
- 710 Bruce, L. C., Frassl, M. A., Arhonditsis, G. B., Gal, G., Hamilton, D. P., Hanson, P. C., Hetherington, A. L., Melack, J. M., Read, J. S., Rinke, K., Rigosi, A., Trolle, D., Winslow, L., Adrian, R., Ayala, A. I., Bocaniov, S. A., Bohrer, B., Boon, C., Brookes, J. D., Bueche, T., Busch, B. D., Copetti, D., Cortés, A., de Eyto, E., Elliott, J. A., Gallina, N., Gilboa, Y., Guyennon, N., Huang, L., Kerimoglu, O., Lenters, J. D., MacIntyre, S., Makler-Pick, V., McBride, C. G., Moreira, S., Özkundakci, D., Pilotti, M., Rueda, F. J., Rusak, J. A., Samal, N. R., Schmid, M., Shatwell, T., Snorthheim, C., Soullignac, F., Valerio, G., van der Linden, L., Vetter, M., Vinçon-Leite, B., Wang, J., Weber, M., Wickramaratne, C., Woolway, R. I., Yao, H., and Hipsey, M. R.: A multi-lake comparative analysis of the General Lake Model (GLM): Stress-testing across a global observatory network, *Environ. Model. Softw.*, 102, 274–291, <https://doi.org/10.1016/j.envsoft.2017.11.016>, 2018a.
- 715 Bruce, L. C., Frassl, M. A., Arhonditsis, G. B., Gal, G., Hamilton, D. P., Hanson, P. C., Hetherington, A. L., Melack, J. M., Read, J. S., Rinke, K., Rigosi, A., Trolle, D., Winslow, L., Adrian, R., Ayala, A. I., Bocaniov, S. A., Bohrer, B., Boon, C., Brookes, J. D., Bueche, T., Busch, B. D., Copetti, D., Cortés, A., de Eyto, E., Elliott, J. A., Gallina, N., Gilboa, Y., Guyennon, N., Huang, L., Kerimoglu, O., Lenters, J. D., MacIntyre, S., Makler-Pick, V., McBride, C. G., Moreira, S., Özkundakci, D., Pilotti, M., Rueda, F. J., Rusak, J. A., Samal, N. R., Schmid, M., Shatwell, T., Snorthheim, C., Soullignac, F., Valerio, G., van der Linden, L., Vetter, M., Vinçon-Leite, B., Wang, J., Weber, M., Wickramaratne, C., Woolway, R. I., Yao, H., and Hipsey, M. R.: A multi-lake comparative analysis of the General Lake Model (GLM): Stress-testing across a global observatory network, *Environ. Model. Softw.*, 102, 274–291, <https://doi.org/10.1016/j.envsoft.2017.11.016>, 2018b.
- 720 Butcher, J. B., Nover, D., Johnson, T. E., and Clark, C. M.: Sensitivity of lake thermal and mixing dynamics to climate change, *Clim. Change*, 129, 295–305, <https://doi.org/10.1007/s10584-015-1326-1>, 2015.
- 725 Couture, R.-M., Moe, S. J., Lin, Y., Kaste, Ø., Haande, S., and Lyche Solheim, A.: Simulating water quality and ecological status of Lake Vansjø, Norway, under land-use and climate change by linking process-oriented models with a Bayesian network, *Sci. Total Environ.*, 621, 713–724, <https://doi.org/10.1016/j.scitotenv.2017.11.303>, 2018.
- Crossman, J., Eimers, M. C., Kerr, J. G., and Yao, H.: Sensitivity of physical lake processes to climate change within a large Precambrian Shield catchment, *Hydrol. Process.*, 30, 4353–4366, <https://doi.org/10.1002/hyp.10915>, 2016.
- 730 Cucchi, M., Weedon, G. P., Amici, A., Bellouin, N., Lange, S., Müller Schmied, H., Hersbach, H., and Buontempo, C.: WFDE5: bias-adjusted ERA5 reanalysis data for impact studies, *Earth Syst. Sci. Data*, 12, 2097–2120, <https://doi.org/10.5194/essd-12-2097-2020>, 2020.
- 735 Danis, P.-A., Von Grafenstein, U., Masson-Delmotte, V., Planton, S., Gerdeaux, D., and Moisselin, J.-M.: Vulnerability of two European lakes in response to future climatic changes, *Geophys. Res. Lett.*, 31, <https://doi.org/10.1029/2004GL020833>, 2004.
- Daufresne, M., Lengfellner, K., and Sommer, U.: Global warming benefits the small in aquatic ecosystems, *Proc. Natl. Acad. Sci. U. S. A.*, 106, 12788–12793, <https://doi.org/10.1073/pnas.0902080106>, 2009.
- 740 Eyring, V., Bony, S., Meehl, G. A., Senior, C. A., Stevens, B., Stouffer, R. J., and Taylor, K. E.: Overview of the Coupled Model Intercomparison Project Phase 6 (CMIP6) experimental design and organization, *Geosci. Model Dev.*, 9, 1937–1958, <https://doi.org/10.5194/gmd-9-1937-2016>, 2016.
- Fernández Castro, B., Bouffard, D., Troy, C., Ulloa, H. N., Piccolroaz, S., Sepúlveda Steiner, O., Chmiel, H. E., Serra Moncadas, L., Lavanchy, S., and Wüest, A.: Seasonality modulates wind-driven mixing pathways in a large lake, *Commun. Earth Environ.*, 2, 1–11, <https://doi.org/10.1038/s43247-021-00288-3>, 2021.

- Ficker, H., Luger, M., and Gassner, H.: From dimictic to monomictic: Empirical evidence of thermal regime transitions in three deep alpine lakes in Austria induced by climate change, *Freshw. Biol.*, 62, 1335–1345, <https://doi.org/10.1111/fwb.12946>, 2017.
- Gaudard, A., Schwefel, R., Raman, L., Schmid, M., Wuest, A., and Bouffard, D.: Optimizing the parameterization of deep mixing and internal seiches in one-dimensional hydrodynamic models: A case study with Simstrat v1.3, *Geosci. Model Dev.*, 10, 3411–3423, <https://doi.org/10.5194/gmd-10-3411-2017>, 2017.
- 750 Gillet, C., Breton, B., Mikolajczyk, T., Bodinier, P., and Fostier, A.: Disruption of the secretion and action of 17,20 $\beta$ -dihydroxy-4-pregnen-3-one in response to a rise in temperature in the Arctic charr, *Salvelinus alpinus*. Consequences on oocyte maturation and ovulation, *Gen. Comp. Endocrinol.*, 172, 392–399, <https://doi.org/10.1016/j.yggen.2011.04.002>, 2011.
- Guillard, J., Gillet, C., and Champigneulle, A.: Revue bibliographique - Principales caractéristiques de l'élevage de l'omble chevalier (*Salvelinus alpinus* L.) en eau douce, *Bull. Fr. Pêche Piscic.*, 47–68, <https://doi.org/10.1051/kmae:1992014>, 1992.
- 755 Hamilton, D. P. and Schladow, S. G.: Prediction of water quality in lakes and reservoirs. Part I — Model description, *Ecol. Model.*, 96, 91–110, [https://doi.org/10.1016/S0304-3800\(96\)00062-2](https://doi.org/10.1016/S0304-3800(96)00062-2), 1997.
- Hipsey, M. R., Bruce, L. C., Boon, C., Busch, B., Carey, C. C., Hamilton, D. P., Hanson, P. C., Read, J. S., de Sousa, E., Weber, M., and Winslow, L. A.: A General Lake Model (GLM 3.0) for linking with high-frequency sensor data from the Global Lake Ecological Observatory Network (GLEON), *Geosci. Model Dev.*, 12, 473–523, <https://doi.org/10.5194/gmd-12-473-2019>, 2019.
- 760 Idso, S. B.: On the concept of lake stability<sup>1</sup>, *Limnol. Oceanogr.*, 18, 681–683, <https://doi.org/10.4319/lo.1973.18.4.0681>, 1973.
- Jane, S. F., Hansen, G. J. A., Kraemer, B. M., Leavitt, P. R., Mincer, J. L., North, R. L., Pilla, R. M., Stetler, J. T., Williamson, C. E., Woolway, R. I., Arvola, L., Chandra, S., DeGasperi, C. L., Diemer, L., Dunalska, J., Erina, O., Flaim, G., Grossart, H.-P., Hambright, K. D., Hein, C., Hejzlar, J., Janus, L. L., Jenny, J.-P., Jones, J. R., Knoll, L. B., Leoni, B., Mackay, E., Matsuzaki, S.-I. S., McBride, C., Müller-Navarra, D. C., Paterson, A. M., Pierson, D., Rogora, M., Rusak, J. A., Sadro, S., Saulnier-Talbot, E., Schmid, M., Sommaruga, R., Thiery, W., Verburg, P., Weathers, K. C., Weyhenmeyer, G. A., Yokota, K., and Rose, K. C.: Widespread deoxygenation of temperate lakes, *Nature*, 594, 66–70, <https://doi.org/10.1038/s41586-021-03550-y>, 2021.
- 765 Jenny, J.-P., Anneville, O., Arnaud, F., Baulaz, Y., Bouffard, D., Domaizon, I., Bocaniov, S. A., Chèvre, N., Dittrich, M., Dorioz, J.-M., Dunlop, E. S., Dur, G., Guillard, J., Guinaldo, T., Jacquet, S., Jamoneau, A., Jawed, Z., Jeppesen, E., Krantzberg, G., Lenters, J., Leoni, B., Meybeck, M., Nava, V., Nöges, T., Nöges, P., Patelli, M., Pebbles, V., Perga, M.-E., Rasconi, S., Ruetz, C. R., Rudstam, L., Salmaso, N., Sapna, S., Straile, D., Tammgeorg, O., Twiss, M. R., Uzarski, D. G., Ventelä, A.-M., Vincent, W. F., Wilhelm, S. W., Wängberg, S.-Å., and Weyhenmeyer, G. A.: Scientists' Warning to Humanity: Rapid degradation of the world's large lakes, *J. Gt. Lakes Res.*, 46, 686–702, <https://doi.org/10.1016/j.jglr.2020.05.006>, 2020.
- 775 Kobler, U. and Schmid, M.: Ensemble modelling of ice cover for a reservoir affected by pumped-storage operation and climate change, *Hydrol. Process.*, 33, <https://doi.org/10.1002/hyp.13519>, 2019.
- Lange, S.: Trend-preserving bias adjustment and statistical downscaling with ISIMIP3BASD (v1.0), *Geosci. Model Dev.*, 12, 3055–3070, <https://doi.org/10.5194/gmd-12-3055-2019>, 2019a.
- 780 Lange, S.: WFDE5 over land merged with ERA5 over the ocean (W5E5) (1.0), <https://doi.org/10.5880/PIK.2019.023>, 2019b.
- Livingstone, D. M.: Impact of Secular Climate Change on the Thermal Structure of a Large Temperate Central European Lake, *Clim. Change*, 57, 205–225, <https://doi.org/10.1023/A:1022119503144>, 2003.
- Mari, L., Garaud, L., Evanno, G., and Lasne, E.: Higher temperature exacerbates the impact of sediments on embryo performances in a salmonid, *Biol. Lett.*, 12, 20160745, <https://doi.org/10.1098/rsbl.2016.0745>, 2016a.
- 785 Mari, L., Garaud, L., Evanno, G., and Lasne, E.: Higher temperature exacerbates the impact of sediments on embryo performances in a salmonid, *Biol. Lett.*, 12, 20160745, <https://doi.org/10.1098/rsbl.2016.0745>, 2016b.
- Mohseni, O., Stefan, H. G., and Eaton, J. G.: Global Warming and Potential Changes in Fish Habitat in U.S. Streams, *Clim. Change*, 59, 389–409, <https://doi.org/10.1023/A:1024847723344>, 2003.
- Moore, T. N., Mesman, J. P., Ladwig, R., Feldbauer, J., Olsson, F., Pilla, R. M., Shatwell, T., Venkiteswaran, J. J., Delany, A. D., Dugan, H., Rose, K. C., and Read, J. S.: LakeEnsemblR: An R package that facilitates ensemble modelling of lakes, *Environ. Model. Softw.*, 143, 105101, <https://doi.org/10.1016/j.envsoft.2021.105101>, 2021.
- 790

- O'Reilly, C. M., Sharma, S., Gray, D. K., Hampton, S. E., Read, J. S., Rowley, R. J., Schneider, P., Lenters, J. D., McIntyre, P. B., Kraemer, B. M., Weyhenmeyer, G. A., Straile, D., Dong, B., Adrian, R., Allan, M. G., Anneville, O., Arvola, L., Austin, J., Bailey, J. L., Baron, J. S., Brookes, J. D., de Eyto, E., Dokulil, M. T., Hamilton, D. P., Havens, K., Hetherington, A. L., Higgins, S. N., Hook, S., Izmest'eva, L. R., Joehnk, K. D., Kangur, K., Kasprzak, P., Kumagai, M., Kuusisto, E., Leshkevich, G., Livingstone, D. M., MacIntyre, S., May, L., Melack, J. M., Mueller-Navarra, D. C., Naumenko, M., Noges, P., Noges, T., North, R. P., Plisnier, P.-D., Rigosi, A., Rimmer, A., Rogora, M., Rudstam, L. G., Rusak, J. A., Salmaso, N., Samal, N. R., Schindler, D. E., Schladow, S. G., Schmid, M., Schmidt, S. R., Silow, E., Soylu, M. E., Teubner, K., Verburg, P., Voutilainen, A., Watkinson, A., Williamson, C. E., and Zhang, G.: Rapid and highly variable warming of lake surface waters around the globe, *Geophys. Res. Lett.*, 42, 10,773-10,781, <https://doi.org/10.1002/2015GL066235>, 2015.
- 795
- 800
- Pagé, C.: Format des données SAFRAN et scénarios climatiques désagrégés au CERFACS, 10, n.d.
- Perga, M.-E., Bruel, R., Rodriguez, L., Guénand, Y., and Bouffard, D.: Storm impacts on alpine lakes: Antecedent weather conditions matter more than the event intensity, *Glob. Change Biol.*, 24, 5004–5016, <https://doi.org/10.1111/gcb.14384>, 2018.
- Piccioni, F., Casenave, C., Lemaire, B. J., Le Moigne, P., Dubois, P., and Vinçon-Leite, B.: The thermal response of small and shallow lakes to climate change: new insights from 3D hindcast modelling, *Earth Syst. Dyn.*, 12, 439–456, <https://doi.org/10.5194/esd-12-439-2021>, 2021.
- 805
- Piccolroaz, S., Toffolon, M., and Majone, B.: A simple lumped model to convert air temperature into surface water temperature in lakes, *Hydrol. Earth Syst. Sci.*, 17, 3323–3338, <https://doi.org/10.5194/hess-17-3323-2013>, 2013.
- Rajwa-Kuligiewicz, A., Rowiński, P., Bialik, R., and Karpiński, M.: Stream diurnal profiles of dissolved oxygen - case studies, 2014.
- 810
- Råman Vinnå, L., Wüest, A., and Bouffard, D.: Physical effects of thermal pollution in lakes, *Water Resour. Res.*, 53, 3968–3987, <https://doi.org/10.1002/2016WR019686>, 2017.
- Råman Vinnå, L., Wüest, A., Zappa, M., Fink, G., and Bouffard, D.: Tributaries affect the thermal response of lakes to climate change, *Hydrol. Earth Syst. Sci.*, 22, 31–51, <https://doi.org/10.5194/hess-22-31-2018>, 2018.
- 815
- Råman Vinnå, L., Medhaug, I., Schmid, M., and Bouffard, D.: The vulnerability of lakes to climate change along an altitudinal gradient, *Commun. Earth Environ.*, 2, 35, <https://doi.org/10.1038/s43247-021-00106-w>, 2021.
- Réalais-Doyelle, E.: Influence de la température sur les premiers stades de vie de trois espèces de poissons dulcicoles : étude de la survie et de la plasticité phénotypique, phdthesis, Université de Lorraine, 2016.
- Riahi, K., van Vuuren, D. P., Kriegler, E., Edmonds, J., O'Neill, B. C., Fujimori, S., Bauer, N., Calvin, K., Dellink, R., Fricko, O., Lutz, W., Popp, A., Cuaresma, J. C., Kc, S., Leimbach, M., Jiang, L., Kram, T., Rao, S., Emmerling, J., Ebi, K., Hasegawa, T., Havlik, P., Humpenöder, F., Da Silva, L. A., Smith, S., Stehfest, E., Bosetti, V., Eom, J., Gernaat, D., Masui, T., Rogelj, J., Strefler, J., Drouet, L., Krey, V., Luderer, G., Harmsen, M., Takahashi, K., Baumstark, L., Doelman, J. C., Kainuma, M., Klimont, Z., Marangoni, G., Lotze-Campen, H., Obersteiner, M., Tabeau, A., and Tavoni, M.: The Shared Socioeconomic Pathways and their energy, land use, and greenhouse gas emissions implications: An overview, *Glob. Environ. Change*, 42, 153–168, <https://doi.org/10.1016/j.gloenvcha.2016.05.009>, 2017a.
- 820
- 825
- Riahi, K., van Vuuren, D. P., Kriegler, E., Edmonds, J., O'Neill, B. C., Fujimori, S., Bauer, N., Calvin, K., Dellink, R., Fricko, O., Lutz, W., Popp, A., Cuaresma, J. C., Kc, S., Leimbach, M., Jiang, L., Kram, T., Rao, S., Emmerling, J., Ebi, K., Hasegawa, T., Havlik, P., Humpenöder, F., Da Silva, L. A., Smith, S., Stehfest, E., Bosetti, V., Eom, J., Gernaat, D., Masui, T., Rogelj, J., Strefler, J., Drouet, L., Krey, V., Luderer, G., Harmsen, M., Takahashi, K., Baumstark, L., Doelman, J. C., Kainuma, M., Klimont, Z., Marangoni, G., Lotze-Campen, H., Obersteiner, M., Tabeau, A., and Tavoni, M.: The Shared Socioeconomic Pathways and their energy, land use, and greenhouse gas emissions implications: An overview, *Glob. Environ. Change*, 42, 153–168, <https://doi.org/10.1016/j.gloenvcha.2016.05.009>, 2017b.
- 830
- Ridout, M. S. and Linkie, M.: Estimating overlap of daily activity patterns from camera trap data, *J. Agric. Biol. Environ. Stat.*, 14, 322–337, <https://doi.org/10.1198/jabes.2009.08038>, 2009.
- 835
- Roberts, J. J., Höök, T. O., Ludsin, S. A., Pothoven, S. A., Vanderploeg, H. A., and Brandt, S. B.: Effects of hypolimnetic hypoxia on foraging and distributions of Lake Erie yellow perch, *J. Exp. Mar. Biol. Ecol.*, 381, S132–S142, 2009a.
- Roberts, J. J., Höök, T. O., Ludsin, S. A., Pothoven, S. A., Vanderploeg, H. A., and Brandt, S. B.: Effects of hypolimnetic hypoxia on foraging and distributions of Lake Erie yellow perch, *J. Exp. Mar. Biol. Ecol.*, 381, S132–S142, <https://doi.org/10.1016/j.jembe.2009.07.017>, 2009b.

- 840 Robertson, D. and Ragotzkie, R.: Changes in the thermal structure of moderate to large sized lakes in response to changes in air temperature, *Aquat. Sci.*, 52, 360–380, <https://doi.org/10.1007/BF00879763>, 1990.
- Saloranta, T. M.: Highlighting the model code selection and application process in policy-relevant water quality modelling, *Ecol. Model.*, 194, 316–327, <https://doi.org/10.1016/j.ecolmodel.2005.10.031>, 2006.
- 845 Saloranta, T. M. and Andersen, T.: MyLake—A multi-year lake simulation model code suitable for uncertainty and sensitivity analysis simulations, *Ecol. Model.*, 207, 45–60, <https://doi.org/10.1016/j.ecolmodel.2007.03.018>, 2007a.
- Saloranta, T. M. and Andersen, T.: MyLake—A multi-year lake simulation model code suitable for uncertainty and sensitivity analysis simulations, *Ecol. Model.*, 207, 45–60, <https://doi.org/10.1016/j.ecolmodel.2007.03.018>, 2007b.
- Schmid, M. and Köster, O.: Excess warming of a Central European lake driven by solar brightening, *Water Resour. Res.*, 52, 8103–8116, <https://doi.org/10.1002/2016WR018651>, 2016.
- 850 Shatwell, T., Thiery, W., and Kirillin, G.: Future projections of temperature and mixing regime of European temperate lakes, *Hydrol. Earth Syst. Sci.*, 23, 1533–1551, <https://doi.org/10.5194/hess-23-1533-2019>, 2019.
- Snorheim, C. A., Hanson, P. C., McMahon, K. D., Read, J. S., Carey, C. C., and Dugan, H. A.: Meteorological drivers of hypolimnetic anoxia in a eutrophic, north temperate lake, *Ecol. Model.*, 343, 39–53, <https://doi.org/10.1016/j.ecolmodel.2016.10.014>, 2017.
- 855 Soares, L. M. V. and Calijuri, M. do C.: Deterministic modelling of freshwater lakes and reservoirs: Current trends and recent progress, *Environ. Model. Softw.*, 144, 105143, <https://doi.org/10.1016/j.envsoft.2021.105143>, 2021.
- Trolle, D., Hamilton, D. P., Hipsey, M. R., Bolding, K., Bruggeman, J., Mooij, W. M., Janse, J. H., Nielsen, A., Jeppesen, E., Elliott, J. A., Makler-Pick, V., Petzoldt, T., Rinke, K., Flindt, M. R., Arhonditsis, G. B., Gal, G., Bjerring, R., Tominaga, K., Hoen, J., Downing, A. S., Marques, D. M., Fragoso, C. R., Søndergaard, M., and Hanson, P. C.: A community-based  
860 framework for aquatic ecosystem models, *Hydrobiologia*, 683, 25–34, <https://doi.org/10.1007/s10750-011-0957-0>, 2012.
- Vinçon-Leite, B., Lemaire, B. J., Khac, V. T., and Tassin, B.: Long-term temperature evolution in a deep sub-alpine lake, Lake Bourget, France: how a one-dimensional model improves its trend assessment, *Hydrobiologia*, 731, 49–64, <https://doi.org/10.1007/s10750-014-1818-4>, 2014.
- van Vuuren, D. P., Edmonds, J., Kainuma, M., Riahi, K., Thomson, A., Hibbard, K., Hurtt, G. C., Kram, T., Krey, V.,  
865 Lamarque, J.-F., Masui, T., Meinshausen, M., Nakicenovic, N., Smith, S. J., and Rose, S. K.: The representative concentration pathways: an overview, *Clim. Change*, 109, 5, <https://doi.org/10.1007/s10584-011-0148-z>, 2011.
- Wetzel, R. G.: *Limnology: Lake and River Ecosystems*, Academic Press, 1024 pp., 2001a.
- Wetzel, R. G.: *Limnology: Lake and River Ecosystems*, Gulf Professional Publishing, 1023 pp., 2001b.
- Williamson, C. E., Saros, J. E., Vincent, W. F., and Smol, J. P.: Lakes and reservoirs as sentinels, integrators, and regulators  
870 of climate change, *Limnol. Oceanogr.*, 54, 2273–2282, [https://doi.org/10.4319/lo.2009.54.6\\_part\\_2.2273](https://doi.org/10.4319/lo.2009.54.6_part_2.2273), 2009.
- Winslow, L., Read, J., Woolway, R., Brenttrup, J., Leach, T., Zwart, J., Albers, S., and Collinge, D.: *rLakeAnalyzer: Lake Physics Tools*, 2019.
- Wolfe, A.: Pourriot, R. et Meybeck, M., sous la direction de, 1995. *Limnologie générale*. Collection d'écologie 25, Masson, Paris, xx + 956 p., ill, tabl., 16,5 × 25 cm. ISBN 2-225-84687-1. Pourriot, R. et Meybeck, M., sous la direction de, 1995.  
875 *Limnologie générale.*, *Géographie Phys. Quat.*, 50, <https://doi.org/10.7202/033095ar>, 1996.
- Woolway, R. I. and Merchant, C. J.: Worldwide alteration of lake mixing regimes in response to climate change, *Nat. Geosci.*, 12, 271–276, <https://doi.org/10.1038/s41561-019-0322-x>, 2019.
- Woolway, R. I., Sharma, S., Weyhenmeyer, G. A., Debolskiy, A., Golub, M., Mercado-Bettín, D., Perroud, M., Stepanenko, V., Tan, Z., Grant, L., Ladwig, R., Mesman, J., Moore, T. N., Shatwell, T., Vanderkelen, I., Austin, J. A., DeGasperi, C. L.,  
880 Dokulil, M., La Fuente, S., Mackay, E. B., Schladow, S. G., Watanabe, S., Marcé, R., Pierson, D. C., Thiery, W., and Jennings, E.: Phenological shifts in lake stratification under climate change, *Nat. Commun.*, 12, 2318, <https://doi.org/10.1038/s41467-021-22657-4>, 2021.